การออกแบบเครื่องปฏิกรณ์เมมเบรนสำหรับปฏิกิริยารีฟอร์มมิ่งด้วยไอน้ำของมีเทนโดยใช้รูปแบบการจัดเรียงตัวของตัวเร่งปฏิกิริยาและเยื่อเลือกผ่านแบบไม่สม่ำเสมอ

นายอัครพล ชีวธารณากร

วิทยานิพนธ์นี้เป็นส่วนหนึ่งของการศึกษาตามหลักสูตรปริญญาวิศวกรรมศาสตรมหาบัณฑิต

สาขาวิชาวิศวกรรมเคมี ภาควิชาวิศวกรรมเคมี

คณะวิศวกรรมศาสตร์ จุฬาลงกรณ์มหาวิทยาลัย

ปีการศึกษา 2555

DESIGN OF MEMBRANE REACTOR FOR STEAM METHANE REFORMING BASED ON NON-UNIFORM CATALYST AND MEMBRANE DISTRIBUTION

Mr. Akkarapon Cheevataranakorn

A Thesis Submitted in Partial Fulfillment of the Requirements
for the Degree of Master of Engineering Program in Chemical Engineering
Department of Chemical Engineering
Faculty of Engineering
Chulalongkorn University
Academic Year 2012

Thesis Title	DESIGN OF MEMBRANE REACTOR FOR STEAM METHANE REFORMING BASED ON NON-UNIFORM CATALYST AND MEMBRANE DISTRIBUTION
By	Mr. Akkarapon Cheevataranakorn
Field of Study	Chemical Engineering
Thesis Advisor	Professor Suttichai Assabumrungrat, Ph.D.
Thesis Co-advisor	Pakorn Piroonlerkgul, D.Eng.

Accepted by the Faculty of Engineering, Chulalongkorn University in Partial Fulfillment of the Requirements for the Master's Degree

……..…..Dean of Faculty of Engineering
(Associate Professor Boonsom Lerdhirunwong, Dr.Ing.)

THESIS COMMITTEE

……Chairman
(Assistant Professor Soorathep Kheawhom, Ph.D.)

……Thesis Advisor
(Professor Suttichai Assabumrungrat, Ph.D.)

……Thesis Co-advisor
(Pakorn Piroonlerkgul, D.Eng.)

…….Examiner
(Pimporn Ponpesh, Ph.D.)

…….External Examiner
(Suwimol Wongsakulphasatch, Ph.D.)

อัครพล ชีวธารณากร: การออกแบบเครื่องปฏิกรณ์เมมเบรนสำหรับปฏิกิริยารีฟอร์มมิ่งด้วยไอน้ำของมีเทนโดยใช้รูปแบบการจัดเรียงตัวของตัวเร่งปฏิกิริยาและเยื่อเลือกผ่านแบบไม่สม่ำเสมอ (DESIGN OF MEMBRANE REACTOR FOR STEAM METHANE REFORMING BASED ON NON-UNIFORM CATALYST AND MEMBRANE DISTRIBUTION) อ. ที่ปรึกษาวิทยานิพนธ์หลัก: ศ.ดร. สุทธิชัย อัสสะบำรุงรัตน์, อ.ที่ปรึกษาวิทยานิพนธ์ร่วม: ดร.ปกรณ์ พิรุณฤกษ์กุล, 76 หน้า

เครื่องปฏิกรณ์เมมเบรนเป็นเครื่องปฏิกรณ์แบบหลายหน้าที่ที่ใช้ในการสังเคราะห์ผลิตภัณฑ์เคมีภัณฑ์และทำให้ผลิตภัณฑ์บริสุทธิ์ในเวลาเดียวกัน นอกจากนี้เครื่องปฏิกรณ์ชนิดนี้ยังสามารถถูกนำไปใช้ในการผลิตไฮโดรเจนผ่านปฏิกิริยารีฟอร์มิงด้วยไอน้ำโดยมีแก๊สมีเทนเป็นสารตั้งต้นได้ด้วยเช่นกัน สำหรับเครื่องปฏิกรณ์เมมเบรนโดยทั่วไปตัวเร่งปฏิกิริยาและเมมเบรนจะถูกจัดเรียงแบบสม่ำเสมอตลอดความยาวของเครื่องปฏิกรณ์ อย่างไรก็ตามรูปแบบของเครื่องปฏิกรณ์เมมเบรนดังกล่าวไม่เหมาะสมสำหรับปฏิกิริยารีฟอร์มมิงของมีเทนเนื่องจากความดันย่อยของไฮโดรเจนบริเวณจุดป้อนสารตั้งต้นมีค่าต่ำมาก มีผลทำให้เมมเบรนในบริเวณดังกล่าวไม่ถูกใช้งานเท่าที่ควร ดังนั้นในงานวิจัยชิ้นนี้จึงนำเสนอการเพิ่มประสิทธิภาพของเครื่องปฏิกรณ์เมมเบรนโดยการเปลี่ยนแปลงการจัดเรียงตัวของตัวเร่งปฏิกิริยาและเมมเบรน โดยในงานวิจัยนี้เครื่องปฏิกรณ์เมมเบรนจะถูกแบ่งเป็นสองส่วนโดยที่แต่ละส่วนจะมีปริมาณตัวเร่งปฏิกิริยาและเมมเบรนแตกต่างกัน อย่างไรก็ตามปริมาณตัวเร่งปฏิกิริยาและเมมเบรนทั้งหมดจะถูกควบคุมให้มีค่าเท่ากันในทุกๆกรณี ปริมาณการเปลี่ยนแปลงของมีเทนและปริมาณการผลิตไฮโดรเจนถูกกำหนดให้เป็นดัชนีชี้วัดสมรรถนะเครื่องปฏิกรณ์เมมเบรน ผลลัพธ์ที่ได้จากการศึกษาในครั้งนี้คือ ในกรณีของเมมเบรนที่มีความสามารถในการแพร่ของไฮโดรเจนผ่านต่ำ ประสิทธิภาพของเครื่องปฏิกรณ์เมมเบรนที่มีการกระจายตัวของเมมเบรนไม่สม่ำเสมอจะมีค่าสูงกว่าประสิทธิภาพของเครื่องปฏิกรณ์ที่มีการกระจายตัวของตัวเร่งปฏิกิริยาและเมมเบรนสม่ำเสมอเป็นอย่างมาก อย่างไรก็ตามการเปลี่ยนแปลงการจัดเรียงตัวของตัวเร่งปฏิกิริยาจะไม่ส่งผลต่อประสิทธิภาพของเครื่องปฏิกรณ์เมมเบรน

ภาควิชา วิศวกรรมเคมี ลายมือชื่อนิสิต .....

สาขาวิชา วิศวกรรมเคมี ลายมือชื่อ อ.ที่ปรึกษาวิทยานิพนธ์หลัก .....

ปีการศึกษา 2555 ลายมือชื่อ อ.ที่ปรึกษาวิทยานิพนธ์ร่วม .....

5470462521: MAJOR CHEMICAL ENGINEERING
KEYWORDS: METHANE STEAM REFORMING / MEMBRANE REACTOR / NON-UNIFORM DISTRIBUTION

AKKARAPON CHEEVATARANAKORN: DESIGN OF MEMBRANE REACTOR FOR STEAM METHANE REFORMING BASED ON NON-UNIFORM CATALYST AND MEMBRANE DISTRIBUTION. ADVISOR: PROF. SUTTICHAI ASSABUMRUNGRAT, Ph.D., CO-ADVISOR: PAKORN PIROONLERKGUL, D.ENG., 76 pp.

Membrane reactor was one of the multifunctional reactors used to simultaneously synthesize and purify a desirable chemical product. It could also be used for hydrogen generation via steam methane reforming reaction. In the conventional membrane reactor, membrane and catalyst were uniformly distributed along the reactor length. This configuration could not actually offer optimum performance since membrane area near the fuel gas entrance was not fully utilized due to low hydrogen partial pressure at the retentate chamber near the gas entrance. By the reason above, the membrane reactor with the distribution of membrane allocation and catalyst distribution were proposed to resolve these issues. In this work, membrane reactor was divided into two sections. Each reactor section contained different catalyst density and membrane area; however, to standardize this study, the total amount of catalyst density and membrane area were kept at constant values. Methane conversion and hydrogen yield were considered as the performance indicators. The results from this study indicated that, as the hydrogen permeability through the membrane was low, non-uniform membrane distribution membrane reactor could offer significantly higher performance compared to uniform distribution membrane reactor. However, the effect of catalyst packing distribution did not significantly affect the performance of non-uniform distribution membrane reactor.

Department: Chemical Engineering Student's Signature .....
Field of Study: Chemical Engineering Advisor's Signature .....
Academic Year: 2012 Co-advisor's Signature .....

ACKNOWLEDGEMENTS

Firstly, the author would like to thank to his advisor, Professor Suttichai Assabumrungrat, Ph.D., for his advices and suggestions in his studying life, study and research. His suggestions enhanced the author to be good person in society with positive thinking, strength and happiness.

Secondly, the author would like to thank to his co-advisor, Pakorn Piroonlerkgul, D.Eng., for the encouragement and suggestions, especially in modeling skills.

Thirdly, the author would like to grateful to Assistant Professor Soorathep Kheawhom, Ph.D, the chairman of thesis committee, Pimporn Ponpesh, Ph.D., and Suwimol Wongsakulphasatch, Ph.D., the examiners, for their useful recommendations.

Furthermore, the author would like to thank his friends in Center of Excellence of Catalysis and Catalytic Reaction Engineering, Department of Chemical Engineering, Faculty of Engineering, Chulalongkorn University for their support, suggestions and coaching until his project became successful.

Finally, the author would like to thank to his parents and sister. They always supported the author everything that they could do. The author could not finish his thesis without their encouragements. The author would like to say he loved his parents.

CONTENTS

LIST OF TABLES

LIST OF FIGURES

FIGURE **PAGE**

CHAPTER I

INTRODUCTION

Due to the continuous growth in world economic, the global fuel consumption, especially fossil fuel, has extremely increased. Inversely, amount of global fossil fuel reservation seems to be decreased due to lower amount of the exploration of the new fuel sources. Owing to the reasons above, the price of fossil fuel has dramatically raised and caused the cost of living to increase. Moreover, the use of the fossil fuel, which is not the renewable source, as the energy source is currently the major cause of the climate change issue owing to the emission of the large amount of greenhouse gas. Unfortunately, traditional energy systems (power plants or vehicles) are characterized as low-efficiency technologies since over 60% of input energy of fossil fuel is lost in these processes [1]. Therefore, to relieve the fuel price crisis and climate change issue, new energy source and more efficient devices would be developed.

Hydrogen is the important raw material for chemical and petrochemical industry, such as ammonia process, processing petroleum, reducing process in metallurgy, hydrogenation of fuels etc.[2] Moreover, Hydrogen is respected as the attractive alternative fuel because of its higher heating value (14.234 kJ/m^3) compared to other types of fuel [3]. Using fuel cell technology, hydrogen could be used as the feedstock for the electricity production via the electrochemical reaction with oxygen. This technology is currently given closely attention due to its high efficiency and environmental friendly.

Unlike fossil fuel, hydrogen cannot be naturally generated and its contents in the atmosphere (0.07%) and surface of the world (0.14%) are very low. At present, 96% of global hydrogen production is from the transformation of fossil fuel feedstock, while the remaining 4% is produced from water splitting process [4, 5]. For the water spitting process, electricity is used to separate water into hydrogen and oxygen. Even though it is easy and clean process, its efficiency is very low due to its high electricity consumption. The widely-used process for hydrogen production is steam methane reforming process. This process is highly endothermic and becomes favored at high temperatures. This process could be divided into three sub-processes. Methane is firstly reformed in the fixed bed reactor at temperature about 973-1173 K to produce hydrogen and carbon monoxide.

To overcome the limitation of thermodynamic equilibrium; large amount of steam is required as the reforming agent to achieve desirable methane conversion and avoid deactivation of the catalyst, because of the coke formation. Suitable steam to carbon ratio for steam reforming reaction is typically between 2 and 4.1. Secondly, the high and low temperature water gas shift reactors are equipped to convert carbon monoxide generated in steam methane reforming reaction to hydrogen to improve hydrogen selectivity. Finally, pressure swing adsorption is used for carbon dioxide separation from hydrogen rich-gas product.

As described in the previous paragraph, since the conventional steam methane reforming process consists of a lot of unit operations, energy loss in the process is also very high. One of the alternative ways to minimize the energy loss in this process is the use of membrane reactor. This reactor is equipped with membrane in order to separate hydrogen from the retentate chamber (reaction zone) in which steam methane reforming reaction takes place. With this bi-functional operation, thermodynamic limitation can be overcame and complete methane conversion with extremely high hydrogen purity can therefore be achieved.

There are two categories of membrane which can be used to separate hydrogen from reformed gas, i.e. the dense membrane such as Palladium membrane, and the porous membrane such as ceramic membrane. The advantage of dense membrane is its higher hydrogen selectivity but the disadvantage is its low hydrogen permeability and high cost. Inversely, the advantage of porous membrane is its high hydrogen permeability, high stability under high-temperature and poisoned operation, and low fabricating cost. However, its hydrogen selectivity is very low. Due to the fact that extremely high purity of hydrogen with very low carbon monoxide content (lower than 10 ppm) is desired for the fuel cell application, palladium membrane which can offer high purity hydrogen production would be the suitable alternative for this application. The conventional membrane reactor is shell and tube type which the tube is made from membrane. The heater is equipped around the shell side in order to supply heat for the endothermic steam methane reforming reaction. Catalyst is uniformly packed inside the tube. The space inside the tube is called “Retentate chamber”, while the space between shell and tube is called “Permeation chamber”. With this configuration, the membrane area and catalyst

cannot be fully utilized. The utilization of catalyst inside the retentate chamber becomes low as the reaction equilibrium is reached while the membrane is not utilized in the zone which the hydrogen partial pressure inside the tube is lower than that outside the tube [6]. Moreover, for highly endothermic or exothermic reaction, the hot spot or cold spot always occurs as the catalyst packing density remains excessively high [1]. Additionally, in case of courter current operation of membrane reactor, back permeation of hydrogen can occur near the entrance of methane gas [7]. Therefore, prior to be used in the large-scale hydrogen production, membrane reactor should be initially studied to optimize its catalyst and membrane utilizations and alleviate the thermal severity of methane steam reforming reaction. In this study, the concept of non-uniform distribution of catalyst weight and membrane area was proposed and evaluated.

1.1 Research objective

In this work, the new configuration of shell and tube membrane reactor was proposed and evaluated using mathematical model. For the newly proposed configuration, the membrane reactor was divided into two sections. Each section was equipped with different membrane area and catalyst packing density, but the values of total membrane area and catalyst weight were controlled to be equal to conventional membrane reactor (uniform membrane area and catalyst packing). The goal of this work was to optimize the membrane area and catalyst packing density of each section in the newly-proposed membrane reactor, and compare its performance with the conventional membrane reactor. In this study, hydrogen yield was used as the performance indicator for benchmarking.

1.2 Scopes of this research

1.2.1. Study the effect of the change in catalyst packing density and membrane area in each section of the newly-proposed membrane reactor on the hydrogen yield

1.2.2. Find the optimum values of the catalyst packing density and membrane area in each section of the newly-proposed membrane reactor

1.2.3. Compare the performance (hydrogen yield) of the newly-proposed membrane reactor with the conventional membrane reactor

1.2.4. Study the effect of two dimensionless numbers (Damköhler number and Peclet number) in order to make the guideline for membrane reactor design.

CHAPTER II

THEORY

2.1 Hydrogen production process

Hydrogen production can be mainly divided into two processes, thermal decomposition of fossil fuel and the decomposition of water. The main products of the thermal decomposition of fossil fuel are hydrogen, carbon monoxide and carbon dioxide, while products of the water decomposition are hydrogen and oxygen.

2.1.1. Thermal decomposition processes

Thermal decomposition process is one of the hydrogen production processes, which uses heat and catalyst to break C-H bonds into hydrogen. Therefore, it must be performed at high temperature. Natural gas, coal, and biomass are generally used as the starting material in this process.

2.1.1.1 Steam reforming.

A steam methane reforming is widely-used for hydrogen production process. This process utilizes high-temperature steam (973–1273 K) as a reactant to produce hydrogen from methane-rich resources, such as natural gas and biogas. Methane firstly reacts with steam under 300–2,500 kPa pressure in the presence of a catalyst to produce hydrogen, carbon monoxide, and a relatively small amount of carbon dioxide (Eq. 2.1). Since steam reforming is endothermic reaction, heat must be supplied to the process for the reaction to proceed. Subsequently, the carbon monoxide and steam are reacted using a catalyst to produce carbon dioxide and additional hydrogen. This reaction is called water-gas shift reaction (Eq. 2.6). Finally, carbon dioxide and other impurities are removed from the gas stream via pressure-swing adsorption process, leaving essentially pure hydrogen. Steam reforming can also be used to produce hydrogen from other fuels like ethanol (Eq. 2.3), propane (Eq. 2.2), and even gasoline (Eq. 2.4-2.5).

Steam-Reforming Reactions

Methane:

$CH_4 + H_2O$ (+heat) → $CO + 3H_2$ (2.1)

Propane:

$C_3H_8 + 3H_2O$ (+heat) → $3CO + 7H_2$ (2.2)

Ethanol:

$C_2H_5OH + H_2O$ (+heat) → $2CO + 4H_2$ (2.3)

Gasoline (using iso-octane and toluene as example compounds from the hundred or more compounds present in gasoline):

$C_8H_{18} + 8H_2O$ (+heat) → $8CO + 17H_2$ (2.4)

$C_7H_8 + 7H_2O$ (+heat) → $7CO + 11H_2$ (2.5)

Water-Gas Shift Reaction

$CO + H_2O$ → $CO_2 + H_2$ (+small amount of heat) (2.6)

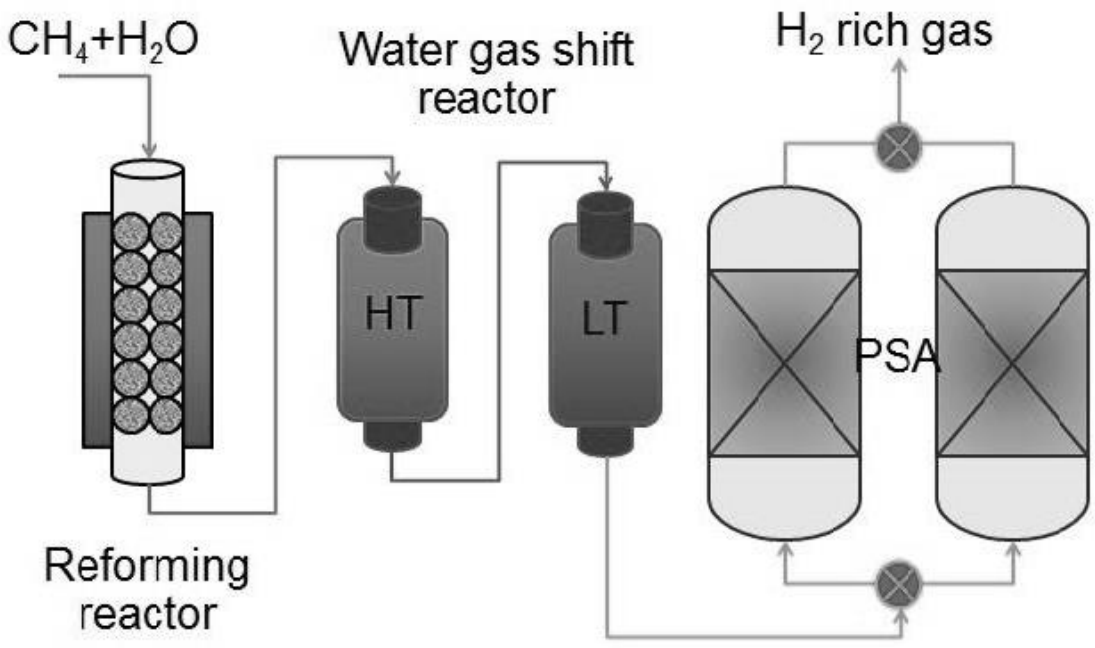

Figure 2.1 Conventional methane steam methane reforming process [2]

2.1.1.2. Partial oxidation.

For the partial oxidation reaction, methane and other hydrocarbons react with a limited amount of oxygen in the reactor chamber (typically, from air). Therefore, it is difficult to produce a complete oxidation of hydrocarbons to carbon dioxide and water.

Operating at this condition, major products derived from partial oxidation reaction contain primarily hydrogen and carbon monoxide (Eq. 2.7-2.11), and a relatively small amount of carbon dioxide and other compounds (Eq. 2.12). There are two types of partial oxidation process, catalytic partial oxidation and thermal partial oxidation [8]. For thermal partial oxidation, it must be operated at temperature of 1573-1773 K to ensure complete conversion [9]. For catalytic partial oxidation, catalyst is used to reduce operating temperature. However, it is difficult for this process to control temperature because of coke generation and hot spot formation [10, 11]. For this process, water gas shift reactor is also included in order to additionally generate hydrogen from carbon monoxide, which is similar to steam reforming process.

Partial oxidation is an exothermic process which large amount of heat is released. Its reaction rate is extremely faster than steam reforming and smaller reactor vessel can therefore be used. As seen in the chemical reaction pathways of partial oxidation (Eq. 2.7 – 2.11), this process offers less hydrogen per unit of the input fuel compared to steam reforming reaction.

Partial Oxidation Reactions

Methane:

$CH_4 + ½O_2 \rightarrow CO + 2H_2$ (+heat) (2.7)

Propane:

$C_3H_8 + 1½O_2 \rightarrow 3CO + 4H_2$ (+heat) (2.8)

Ethanol:

$C_2H_5OH + ½O_2 \rightarrow 2CO + 3H_2$ (+heat) (2.9)

Gasoline (using iso-octane and toluene as example compounds from the hundred or more compounds present in gasoline):

$C_8H_{18} + 4O_2 \rightarrow 8CO + 9H_2$ (+heat) (2.10)

$C_7H_8 + 3½O_2 \rightarrow 7CO + 4H_2$ (+heat) (2.11)

Water-Gas Shift Reaction

$CO + H_2O \rightarrow CO_2 + H_2$ (+small amount of heat) (2.12)

2.1.2. Water decomposition

Using the water decomposition process, which is so-called electrolysis process, electricity is supplied so as to split water into hydrogen and oxygen. This process takes place in an electrolyzer which consists of an anode and a cathode separated from each other by an electrolyte or a membrane like fuel cell. Production of Hydrogen via this process can result in zero greenhouse gas emissions, depending on the source of the electricity used. To evaluate the benefits of hydrogen production via electrolysis, the electricity cost, the electricity generation efficiency and also greenhouse gas emission resulting from electricity generation must be considered.

2.1.2.1. PEM electrolyzer

In a polymer electrolyte membrane (PEM) electrolyzer, the electrolyte is a solid specialty plastic material. Water reacts at the anode to form oxygen and positively charged hydrogen ions (protons) (Eq. 2.13) [9]. The electrons flow through an external circuit and the hydrogen ions selectively move across the PEM to the cathode [9]. At the cathode, hydrogen ions react with electrons from the external circuit to form hydrogen gas (Eq. 2.14).

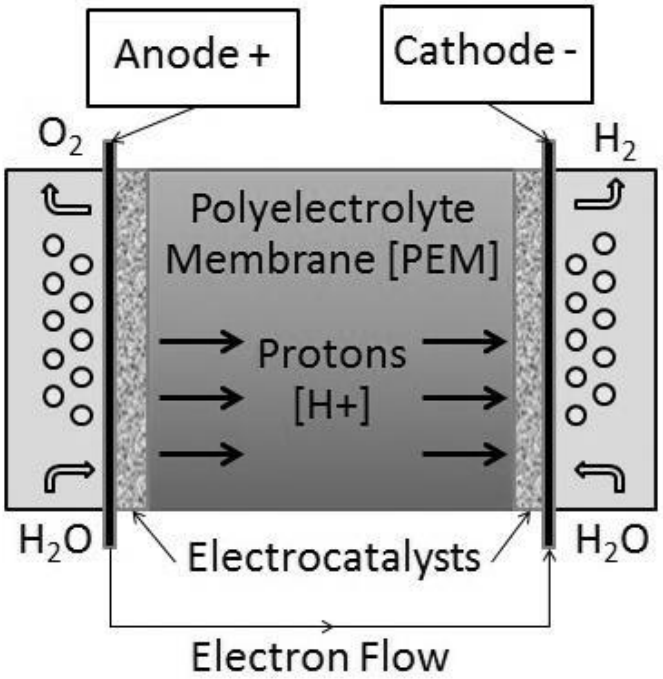

Figure 2.2 Polymer electrolyte membrane electroyzer [12]

Anode Reaction: $2H_2O \rightarrow O_2 + 4H^+ + 4e^-$ (2.13)

Cathode Reaction: $4H^+ + 4e^- \rightarrow 2H_2$ (2.14)

2.1.2.2. Alkaline Electrolyzers

Alkaline electrolyzers are similar to PEM electrolyzers; however, an alkaline solution (sodium or potassium hydroxide) is used as the electrolyte [13]. These electrolyzers have been commercially applied for many years.

2.1.2.3. Solid Oxide Electrolyzers

Solid oxide electrolyzers, which use a solid ceramic material that selectively transmits negative-charge oxygen ions at elevated temperatures as the electrolyte, generate hydrogen in a slightly different way compared to other electrolyzers. Water at the cathode reacts with electrons from the external circuit to form hydrogen gas and oxygen ions [9]. The oxygen ions permeate through the membrane and react at the anode to form oxygen gas and release the electrons to the external circuit [9]. Solid oxide electrolyzers must be operated at extremely higher temperature 773 K – 1073 K compared to PEM electrolyzers which are operated at 353 K – 373 K, and alkaline electrolyzers which are operated at 373 K – 423 K. The solid oxide electrolyzers can effectively utilize available heat at these elevated temperatures (from various sources, including nuclear energy) to decrease the amount of electrical energy required to produce hydrogen from water.

2.2 Membrane reactor for hydrogen production

From the previous section, there are many pathways to produce hydrogen. Although steam reforming of natural gas is the most popular pathway to produce hydrogen, there are some disadvantages for this process. For example, high operating temperature and pressure are provided to achieve completely methane conversion. Membrane reactor is the alternative technology which can enhance the performance of steam methane reforming process. This reactor is equipped by hydrogen selective membrane which is used to separate hydrogen from the retentate chamber. With its

operation, the reaction equilibrium of steam methane reforming and water-gas shift reactions are shifted forward due to the removal of H_2 gas, which are product of these reactions.

2.2.1. Membrane for hydrogen production

Most of hydrogen selective membranes operate based on the principle that only hydrogen can penetrate through the membrane because of the inherent properties of the material. The permeability of hydrogen through the membrane depends on the type of membrane. The operation of H_2-selective membrane relies on the difference of hydrogen partial pressure between retentate and permeation chambers as the driving force for H_2 permeation.

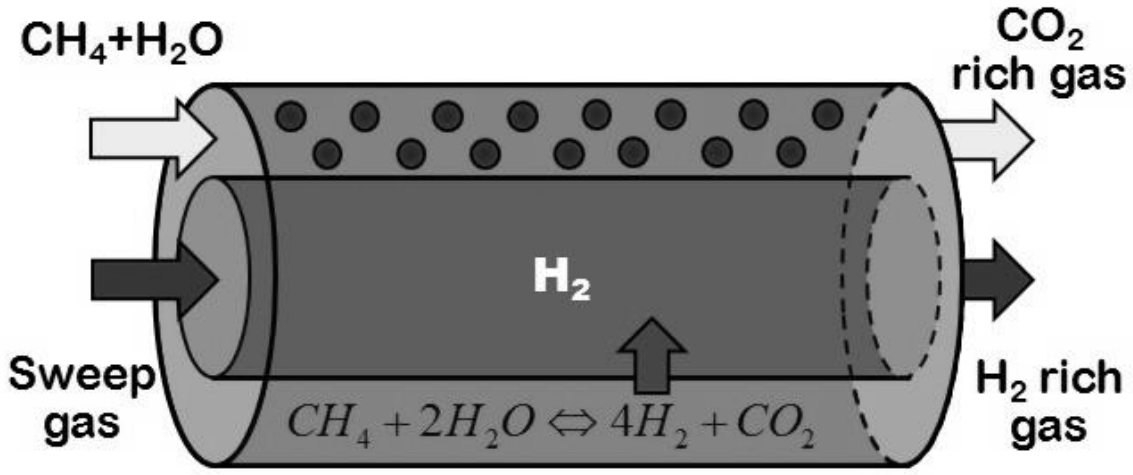

Figure 2.3 Membrane reactor [14]

2.2.2. Palladium membrane

Palladium is the material which can absorb large amount of hydrogen at room temperature and atmospheric pressure. H_2 absorption takes place in the octahedral side in face center cubic lattice [15]. Palladium would be in hydride form in the ambient temperature [16]. High hydrogen selectivity, fast sorption kinetic and reversibility properties of hydride structure offers the advantage to palladium as the suitable material for H_2-selective membrane. Only hydrogen can diffuse through the palladium membrane as there is the difference in H_2 partial pressure between each membrane side. The

palladium membrane is typically a metallic tube comprising a palladium and silver alloy material possessing the unique property of allowing only monoatomic hydrogen to pass through its crystal lattice when it is heated above 573 K. The hydrogen gas molecule coming into contact with the palladium membrane surface dissociates into monatomic hydrogen and passes through the membrane. On the other surface of the palladium membrane, the monatomic hydrogen is recombined into molecular hydrogen.

Figure 2.4 Palladium membrane [17]

2.2.3 Limitation of Palladium membrane

2.2.3.1. The adsorption of H_2 below its critical point

The critical point of palladium membrane is 571 K and 2 MPa. If it is operated under a critical point, two palladium phases (α, β) will be occurring [18]. Both of them keep palladium membrane in the form of face center cubic; however, the unit cell parameter increase from 0.3890 nm (pure Pd) to 0.895 nm (α phase) and 0.410 nm (β phase) at room temperature [18, 19]. The α- phase will be occurred as H/Pd ratio is low and the β phase will be occurred as H/Pd ratio is high. The change of volume of Pd due to the phase transformation is the cause of bulk and grain boundary defects.

2.2.3.2. Hydrogen embrittlement

Hydrogen embrittlement can occur as Pd losses its ductility because of H_2 exposure and causes metal cracking [20].

2.2.3.3. Deactivation form carbon and poison

The surface deactivation of Pd membrane can occur as it is exposed to unsaturated hydrocarbon and poisoned gas, e.g. sulfur, CO [21].

2.2.4. The solution to alleviate these limitations

Use Pd-alloy instead of pure Pd

When Pd-alloy is used, its critical temperature increases and the occurrence of Pd-state with different lattice sizes of α and β become more difficult for Pd-alloy compared to pure Pd [19]. Moreover, Pd-alloy membrane could be operated at lower operating temperature compared to pure Pd due to its higher H_2 permeation rate due to the increase in the bond distance for the alloy form. Also, Pd-membrane is not prone to sulfur as it is in the alloy form.

2.3 The Mechanism of Hydrogen Diffusion

The hydrogen permeation mechanism through composite palladium membranes can be explained by two theories: (a) a traditional solution–diffusion mechanism for dense membranes, and (b) a Knudsen diffusion mechanism or combined mechanism of Knudsen diffusion and surface diffusion for porous membranes. For the solution–diffusion mechanism, the hydrogen transportation through a palladium layer is composed of the 7 following sub-steps [22]:

1) Adsorption of hydrogen molecules on the high hydrogen partial pressure side of the membrane surface.

2) Dissociation of hydrogen molecules on the same surface. Its super dissociative property is similar to catalyst.

3) The chemisorbed molecule dissociates into atomic, consisting of a proton and an electron. Unlike other metal, Palladium does not have activation barrier. Therefore, energy input is not required for hydrogen transfer process.

4) The dissociated hydrogen atoms dissolve into the lattice of the metal. It is adsorbed in the octahedral side in face center cubic lattice to form metal Hydride.

5) The dissociated hydrogen atoms diffuse through the lattice from the membrane surface side with higher hydrogen partial pressure to the membrane surface side with lower hydrogen partial pressure.

6) At the membrane surface side with lower hydrogen partial pressure, the proton and electron recombine into hydrogen molecules.

7) The hydrogen molecule desorbs from the membrane surface side with lower hydrogen partial pressure to the bulk gas.

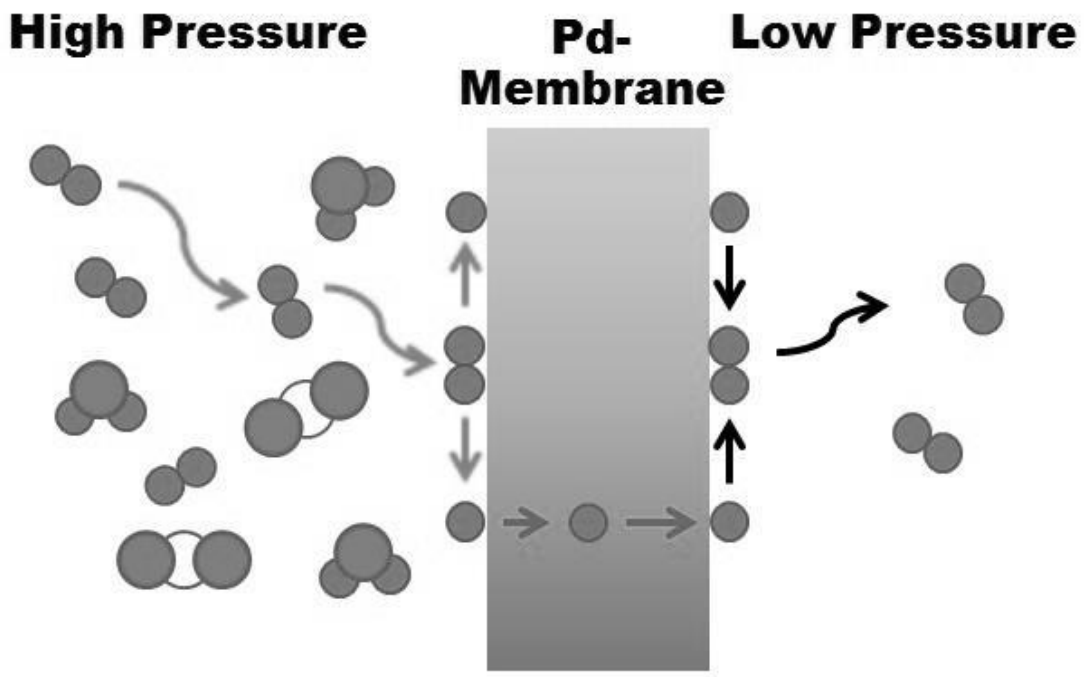

Figure 2.5 Mechanism for hydrogen transport in palladium membrane [23]

CHAPTER 3

LITERATURE REVIEW

Nowadays, a lot of researches have focused on membrane reactor design and optimization. Because membrane reactor used lower energy and offered higher conversion compared to the conventional reactor, it is an alternative way for several chemical production processes. Many researches on membrane reactor were aimed at the optimization of the operating conditions (temperature, pressure, reactant concentration, etc.), reactor size and production cost, especially for small mobile applications [24] .

There are many researches demonstrating the simulation of steam methane reforming in membrane reactor. Most of the models would use kinetic equations given in Xu and Froment's work [25]. Isothermal and isobaric models were the simple models used to explain the process behavior. However, the accuracy achieved from the modeling using these assumptions is not adequate because of highly endothermic behavior of steam methane reforming reaction. Nowadays, there are several developments of non-isothermal model for the study of the operation of steam methane reforming membrane reactor.

Marigliano, et al. [14] investigated the effect of heat transfer of membrane reactor. Because membrane reactor was the shell and tube type, the position of catalyst was in the membrane or in the annulus. One-dimensional analysis with material and energy balance calculations was performed to describe the behavior of membrane reactor. Sievert's law was used to describe the behavior of Pd-based membrane. The results showed that the temperature drop of membrane reactor which the catalyst was packed inside the membrane tube was more than that catalyst packing is in annular zone of membrane due to higher thermal resistance of the former. Therefore, the annular catalyst-packed membrane reactor was expected to offer higher efficiency.

Yu [26] studied the simulation of porous ceramic membrane reactor. Also, one-dimensional mass and energy calculations were used for the simulation. The goal of this research was to compare the efficiency of the membrane steam reforming reaction as the different types of sweep gas were used. The results showed that, as steam was used as sweep gas, the steam partial pressure at the reaction side slightly decreases compared

with the case that nitrogen was used as sweep gas. It could be concluded that the performance of membrane reactor, which steam was used as the sweep gas, was higher than that of membrane reactor, which N_2 was used as the sweep gas since reactant consumption of the former was slightly higher.

Many recent researches focused on the effect of catalyst weight, reactant feed rate and membrane area on the membrane reactor performance. The cost of catalyst and membrane module was the major cost of membrane reactor production. In many works, the reaction rate was represented by Damkohler's number (*Da*) and permeation rate was represented in term of permeation number (*Pe*). These two dimensionless numbers will be used to design membrane reactor. Moon and Park [27] studied the effect of the change in the permeation rate, reaction rate and selectivity in porous membrane reactor and provided the guideline for membrane reactor design. Two dimensionless groups, *Pe* and *Da*, were used to represent the magnitude of permeation rate and reaction rate. The results showed that four distinctive regions, where the conversion was controlled by different mechanisms, were identified. The maximum methane conversion of a membrane reactor, which is the equilibrium conversion based on the assumption that H_2 partial pressure in permeate side was equal to that in reaction side, could be achieved as *Pe* was equal to 0 and *Da* was greater than 10. The permeation rate was the rate-limiting mechanism when *Pe* was between 0.1 and 10.

Boutikos and Nikolakis [28] investigated the performance of a water gas shift membrane reactor in term of CO conversion and hydrogen recovery. The effects of membrane permselectivity, permeation flux and reaction rate were investigated. The reactor configuration used in this work was isothermal shell and tube reactor. The result showed that CO conversion increased when the permselectivity increased. Maximum CO conversion was achieved as Damkhöler number (*Da*) was equal to the permeation number (*Pe*).

Gómez-García et al. [29] investigated the performance of ammonia decomposition membrane reactor. One dimensional isothermal model would be used for shell and tube configuration. Performance chart was constructed in order to explain the effect of permeation rate and reaction rate on the reactor perfomance. The maximum conversion

was achieved as the value of log(*Pe*) was between 1.5 and 2 and the value of log(*Da*) was between -0.5 and 0.

Chiappetta et al. [30] evaluated the performance of membrane reactor. The design parameters considered in this evaluation were membrane surface area (A_m), catalyst volume (V_{cat}), methane load in feed (L_s) and gas hourly space velocity (GHSV). The results showed that two-time increase of the methane conversion has been obtained by enhancing the ratio of A_m to V_{cat} from 0.42 to 2.1 cm^2cm^{-3}. Ultimate methane conversion of the 68% and hydrogen recovery approximately of 43% were achieved as A_m to V_{cat} ratio was 2.1 cm^2cm^{-3} and L_s to A_m ratio was 8.4 cm^3(STP) $cm^{-2}min^{-1}$ as operating pressure was equal to 800 kPa.

Lin et al. [31] studied the displacement of methane conversion in the steam methane reforming. They studied the effect of weight hourly space velocity (WHSV) and load-to-surface ratio on the performance of membrane reactor. The results showed that the lower load-to-surface ratio or WHSV was, the higher the conversion of methane. The recovery yield of hydrogen decreased with the increase in load-to-surface ratio. As WHSV was below 3 h^{-1}, the conversion reached its equilibrium status (58%) and could not be further enhanced via the reduction of WHSV. In case that the conversion approached the equilibrium, load-to-surface ratio was less than 0.2 m/h.

Mender et al. [32] performed experimental and modeling researches of water-gas shift reaction at low operating temperature. The finger-like configuration was used to evaluate the performance which was investigated in term of Damkohler's number and contact time. One-dimentional isothermal model considering pressure drop in the reactor was developed in this research. The effects of the change in temperature, space velocity, feed pressure and permeate side mode (vacuum or sweep gas) were studied. The results showed that high performance should be got from this configuration for some operating conditions.

The distribution of the catalyst packing and membrane density were also the critical issue for the design of the membrane reactor. In some reactor zone, the dense catalyst packing or membrane area was not required due to low reaction rate or low H_2 permeation. Therefore, new membrane reactor configuration should be developed to

achieve suitable catalyst packing and membrane area which offer optimum reactor efficiency.

For courter-current operation of membrane reactor, there were some problems near methane feeding position inside the membrane reactor. The hydrogen partial pressure at this position of reaction side was at minimum value because the reaction did not start occurring. So, the back permeation was found in this position. By the reason above, membrane area was not necessary for this position. There were many researches focusing in the courter-current configuration of membrane reactor. Piemonte et al. [7] studied the courter-current configuration membrane reactor for water-gas shift reaction. Because the conversion of carbon monoxide was low at the first part of the membrane reactor, the installation of the membrane module into the first part of the reactor was not required. It was demonstrated that the permeated H_2 flow rate per membrane surface (average membrane flux) strongly improved when selective membrane was placed only in the second part of the reactor.

Lima et al. [33] studied the performance of membrane reactor in co-current and courter-current operating modes. The results showed that counter-current configuration offered better performance compared to co-current configuration. An optimization problem was formulated and solved to find the optimal membrane reactor design for water gas shift reaction. The optimization results showed that the optimal solution of reactor design should consist of the first section of catalytic reactor without membrane installation followed by the second reactor installed with membrane module. With this configuration, 25% cost saving in the membrane module cost was achieved.

Barbieri et al. [34] studied the performance of membrane reactor without the feed of sweep gas into the permeation side. Using this configuration, back permeation was found in the initial part of the membrane reactor. So they proposed the installation of the membrane only in the second path of the catalytic bed so as to achieve full exploitation of membrane.

Some recent researches also focused on the optimization of the distribution of membrane and catalyst in axial direction of membrane reactor. Unless the system reached thermodynamic equilibrium, its performance will depend on kinetic of reaction rate and

permeation rate. Li et al. [35] used the concept of the staged-separation membrane reactor to improve the performance of membrane reactor. The advantage of new configuration was its super-equilibrium conversion when reaction zone and separation zone was separated. In this work, steam methane reforming for hydrogen production was used as the example to prove the concept of the staged-separation membrane reactor. Normally, due to the fact that the steam methane reforming is an endothermic reaction, it is favored to be operated at high temperature. Even though hydrogen flux increases when temperature increases, the stability of membrane decreases. If it was operated at low temperature, its stability was high and membrane thickness can therefore be reduced. Therefore, the suitable condition for stage-separation membrane reactor for steam methane reforming was high temperature at reaction zone and low temperature at membrane zone. It could be also concluded from this work that the performance of the staged-separation membrane reactor was higher compared with those of a conventional membrane reactor and a traditional reformer together with an ex-situ membrane purifier. Compared with the conventional membrane reactor, the metal cost of palladium-based membranes decreases by 86.5% and the membrane area decreases by more than 70% for stage-separation membrane reactor to achieve equal hydrogen production capacity.

Moreover, Li et al. [36] investigated the staged separation membrane reactor configuration for the steam methane reforming reaction using oxygen as a reforming agent. In the reactor, catalyst and membrane section were separated from each other in order to operate at suitable condition to get better overall performance. In catalyst section, thermodynamic equilibrium approach was assumed and oxygen was fed into the reaction section. The modeling results also showed that super-equilibrium conversion of methane could be achieved in this reactor combination. The performance of the reactor was affected by the allocation of membrane module in each reactor section. About 55% of the total membrane module should be located in the first section for all conditions studied.

Caravella et al. [6] studied the optimization of catalyst and membrane area axial distributions using Matlab. A configuration of a permeative-stage membrane reactor (PSMR) consisting of the series of traditional reactive and membrane permeative stages was used. The calculation was based on one-dimensional mass, momentum and energy balances considering thermal effects on all the system properties. Firstly, an equisized-nine-stage PSMR was analyzed at various temperature and membrane thicknesses, in

comparison with a conventional membrane reactor. The results showed that the conversion could be improved from 0.93 to 0.97, while the recovery factor increased from 0.60 to 0.73. Then, two optimization problems would be solved so as to get the stage lengths as design variables. Two objective functions for optimization problems were to maximize the methane conversion and the hydrogen recovery. The results showed that PSMR offered higher conversion and lower recovery factor for the case of maximum methane conversion, while the opposite situation occurred when the recovery factor was maximized. In the case of adiabatic operation in the permeative state, the recovery factor of PSMR factor was about 21% higher than that of conventional membrane reactor for the optimization using maximum hydrogen recovery factor as objective function. Therefore, the conclusion for this paper showed that the reactive/permeative stage distribution had to be considered as an important reactor design parameter.

The catalyst packing distribution in the catalytic reactor was also widely studied in the recent researches. When the reaction occurred, the issue about hot and cold spot would be considered. Their disadvantages were the cracking of reactor wall or membrane and coking. The decrease in catalyst packing density could relieve the issue of hot or cold spot; however, the yield of reaction also decreased. Therefore, the density catalyst packing should be also carefully considered for both conventional and membrane reactors.

Hwang and Smith [37] used inert pellets and side-stream feeding to decrease temperature profile of conventional reactor. Nitrobenzene hydrogenation and ethylene oxidation in non-isothermal and non-adiabatic reactors were considered in this study. The results showed that higher reactor performance, characterized by conversion, yield or selectivity, could be achieved with optimal temperature profiles manipulated by side-streams and inert pellets. In the case of nitrobenzene hydrogenation, the concept of catalyst dilution with inert material could control temperature profile effectively. Complete conversion was achieved with temperature range 475-725 K. For side stream feeding, complete conversion was achieved with temperature range 475-733 K. For ethylene oxidation reaction, the reaction yield increased from 16.5% to 47.5%, using the concept of catalyst dilution.

Chiappetta et al. [1] used the concept of non-uniform catalyst distribution for exothermic reaction. Two-dimensional model was used to describe the behavior of

membrane reactor. Water gas shift reaction was the example of endothermic reaction for this consideration. Three cases of non-uniform catalyst weight distribution (uniform, linear increasing and exponential increasing) were used for finding the optimal configuration. The results showed that linearly-increase catalyst distribution along the membrane reactor offered higher capability in controlling the temperature profile compared to an exponential catalyst distribution. However, at high pressures (2000 kPa) the advantage of a linear catalyst distribution was not observed, it showed superior performance to an exponential catalyst distribution at 500 and 110 kPa.

Caravella et al. [38] also proposed the new configuration of membrane reactor. In their previous work, they found the permeative-stage membrane reactor (PSMR) which offered higher performance than conventional membrane reactor. But its disadvantage was its inflexibility operating since it was suitable for particular condition. So, the reactor configuration with reactive/permeative stages in series with inert/permeative stages was proposed. The optimum length of each reactor stage was found and two performance indicators, methane conversion and hydrogen recovery yield, were selected. The system was studied considering co- and counter-current flow conditions. The results showed that the counter-current flow always offered better performances than the co-current flow operation. An almost equi-sized distribution was achieved by maximizing the hydrogen recovery factor in both flow configurations, whereas, when methane conversion was maximized, the optimization procedure provided a negligible last inert stage. The performances of the ten-stage membrane reactor were significantly higher than the one of the reference membrane reactor (two-stage one) in terms of methane conversion and hydrogen recovery. It could be concluded that the number of stages were the most important variable affecting the worthwhile utilization of catalyst.

Caravella et al. [39] also studied about the influence of the number of stages, and the amount of catalyst on the performance of membrane reactor. The membrane reactor with reactive and inert stages in series would be compared with a conventional membrane reactor in term of a methane conversion, hydrogen yield and hydrogen recovery yield. The results showed that steam methane reforming membrane reactor which contained high number of stages offered equal performance compared to a reactor with uniformly catalyst packing diluted with inert particles. The proposed configuration with a sufficiently high number of stages and significantly smaller catalyst amounts (up to 70%

lower) could achieve comparable performance to the conventional catalytic steam reforming in all considered operating conditions.

CHAPTER IV

MATHEMATICAL MODEL

4.1 Configuration of membrane reactor

Shell and tube membrane reactor was used in this work. The wall of reactor was covered with furnace to heat the system. Two kinds of tube, Pd-based membrane and stainless steel, were packed inside the reactor. The catalyst and inert particles were installed in annulus side, which was called retentate chamber. Methane and steam were fed into the retentate chamber as the reactants. In the membrane tube which was called permeation chamber, the vacuum operation mode was performed to achieve high hydrogen permeation rate through the membrane.

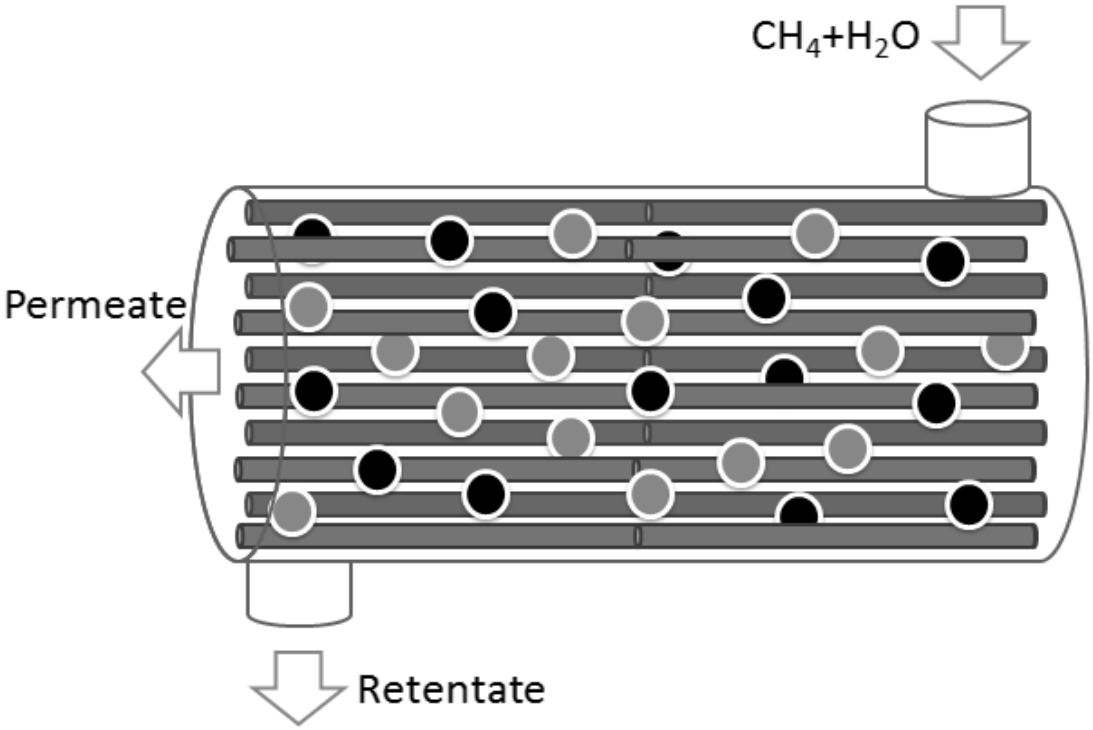

Figure 4.1 Uniform membrane and catalyst distribution membrane reactor

4.1.1. Non-uniform membrane area and catalyst weight distribution

For this configuration, membrane reactor was divided into 2 sections. Each section contains different amount of catalyst and membrane areas. However, the total amount of catalyst and membrane area was controlled to be similar for every scenario. In this study, membrane area would be diluted with stainless steel tube and catalyst would be diluted with inert particle to control the catalyst density and membrane area in each section. To evaluate the performance of the new proposed membrane reactor, the conventional membrane reactor with uniform distribution configuration was considered as a base case.

4.1.2. Guideline for membrane reactor design

Since two design parameters, methane feed flow rate to catalyst weight ratio and methane feed flow rate to membrane area were very important factors affecting performance of the new proposed configuration of membrane reactor, the guideline for the new membrane reactor design was proposed in this study to find out the optimum values of these two parameters. Damkohler number and Peclet number were calculated to be a representative of the ratio of methane feed flow rate to catalyst weight and the ratio of reactant feed flow rate to membrane area, respectively. The methane conversion and hydrogen yield were calculated using Eqs. 4.1-4.2 and considered as performance indicators in this study.

$$X_{CH_4} = \frac{(F_{CH_4,initial} - F_{CH_4})}{F_{CH_4,initial}} \times 100\% \quad (4.1)$$

$$Yield_{H_2} = \frac{(F_{H_2,Permeation})}{4 * F_{CH_4,initial}} \times 100\% \quad (4.2)$$

4.2 Mathematical model for calculation

4.2.1 Reaction rate expressions

Three chemical reactions, steam methane reforming reaction (Eq. (4.3)), water-gas shift reaction (Eq. (4.4)) and carbon dioxide methanation reaction (Eq. (4.5)) were considered to occur in the membrane steam reforming reactor.

$$CH_4 + H_2O \Leftrightarrow CO + 3H_2 \qquad \Delta H^o_{298K} = 260\,\text{kJ/mol} \tag{4.3}$$

$$CO + H_2O \Leftrightarrow CO_2 + H_2 \qquad \Delta H^o_{298K} = -41\,\text{kJ/mol} \tag{4.4}$$

$$CH_4 + 2H_2O \Leftrightarrow CO_2 + 4H_2 \qquad \Delta H^o_{298K} = 165\,\text{kJ/mol} \tag{4.5}$$

The rate expressions for these reactions (Eqs. (4.3)–(4.5)) were obtained from Xu and Froment's work [25] as given in Eqs. (4.6)-(4.9). The unit of reaction rate was mol(hkg$_{Cat}$)$^{-1}$. The equations used to calculate adsorption equilibrium constants, reaction rate constants, chemical equilibrium constants and dimensionless reaction rate were given in Eqs. (4.10)-(4.13), Eqs. (4.14)-(4.16), Eqs. (4.17)-(4.19) and Eqs. (4.20)-(4.22), respectively.

$$\Re_1 = \frac{k_1}{P_{H_2}^{2.5}} \frac{\left(P_{CH_4} P_{H_2O} - \dfrac{P_{H_2}^3 P_{CO}}{K_{equilibrium(1)}} \right)}{DEN^2} \tag{4.6}$$

$$\Re_2 = \frac{k_2}{P_{H_2}} \frac{\left(P_{CO} P_{H_2O} - \dfrac{P_{H_2} P_{CO_2}}{K_{equilibrium(2)}} \right)}{DEN^2} \tag{4.7}$$

$$\Re_3 = \frac{k_3}{P_{H_2}^{3.5}} \frac{\left(P_{CH_4} P_{H_2O}^2 - \dfrac{P_{H_2}^4 P_{CO_2}}{K_{equilibrium(3)}} \right)}{DEN^2} \tag{4.8}$$

$$DEN = 1 + K_{CO} P_{CO} + K_{H_2} P_{H_2} + K_{CH_4} P_{CH_4} + K_{H_2O} \frac{P_{H_2O}}{P_{H_2}} \tag{4.9}$$

$$K_{CH_4} = 6.65 \times 10^{-6} \exp\left(\frac{4604}{T} \right) \ \text{kPa}^{-1} \tag{4.10}$$

$$K_{H_2O} = 1.77 \times 10^{5} \exp\left(\frac{-1066.35}{T}\right) \quad (4.11)$$

$$K_{H_2} = 6.12 \times 10^{-11} \exp\left(\frac{9971.13}{T}\right) \text{ kPa}^{-1} \quad (4.12)$$

$$K_{CO} = 8.23 \times 10^{-7} \exp\left(\frac{8497.71}{T}\right) \text{ kPa}^{-1} \quad (4.13)$$

$$k_1 = 4.2248 \times 10^{19} \exp\left(\frac{-28879}{T}\right) \text{ mol.kPa}^{0.5}\text{/kgCat.hr} \quad (4.14)$$

$$k_2 = 1.955 \times 10^{7} \exp\left(\frac{-8074.3}{T}\right) \text{ mol.kPa}^{-1}\text{/kgCat.hr} \quad (4.15)$$

$$k_3 = 1.0202 \times 10^{19} \exp\left(\frac{-29336}{T}\right) \text{ mol.kPa}^{0.5}\text{/kgCat.hr} \quad (4.16)$$

$$K_{equilibrium(1)} = 1.198 \times 10^{17} \exp\left(\frac{-26830}{T}\right) \text{ kPa}^{2} \quad (4.17)$$

$$K_{equilibrium(2)} = 1.767 \times 10^{-2} \exp\left(\frac{4400}{T}\right) \quad (4.18)$$

$$K_{equilibrium(3)} = 2.117 \times 10^{15} \exp\left(\frac{-22430}{T}\right) \text{ kPa}^{2} \quad (4.19)$$

$$R_1 = \frac{\Re_1 \times \sqrt{P}}{k_1^o} \quad (4.20)$$

$$R_2 = \frac{\Re_2 \times \sqrt{P}}{k_1^o} \quad (4.21)$$

$$R_3 = \frac{\Re_3 \times \sqrt{P}}{k_1^o} \quad (4.22)$$

4.2.2 The permeation rate

Hydrogen flux through the Pd/Ag membrane was described by the Sievert's law (Eq. (4.23)).

$$J_{H_2} = \frac{B_H}{\delta}\left(\sqrt{P_{H_2}} - \sqrt{P_{H_2}^{perm}}\right) \quad (4.23)$$

The Arrhenius expression for Hydrogen Flux was reported by F. Gallucci et al. [40] as shown in Eq. (4.24).

$$B_H = 1.27503 \times \exp\left(\frac{-29160}{8.314 \times \left(\frac{T + T_{perm}}{2}\right)}\right) \quad \text{mol.m/(h.m}^2\text{.kPa}^{0.5}\text{)} \quad (4.24)$$

To be easily compared to other works, dimensionless Hydrogen flux was calculated as shown in Eq. (4.25).

$$J_{H_2}^{*} = \frac{J_{H_2} \times \delta}{B_H^o \times \sqrt{P}} \quad (4.25)$$

4.2.3 Overall mathematical model used in this work

In this work, material and energy balances were performed and the conversion and productivity terms of each chemical substance are calculated using Eqs. (4.26)-(4.31).

$$X_{CH_4} = 1 - \frac{F_{CH_4}}{F_{CH_4}^0} \quad (4.26)$$

$$X_{H_2O} = m - \frac{F_{H_2O}}{F_{CH_4}^0} \quad (4.27)$$

$$X_{CO} = \frac{F_{CO}}{F_{CH_4}^0} \quad (4.28)$$

$$X_{CO_2} = \frac{F_{CO_2}}{F_{CH_4}^0} \quad (4.29)$$

$$X_{H_2} = \frac{F_{H_2}}{F_{CH_4}^0} \quad (4.30)$$

$$Y_{H_2} = \frac{F_{H_2}^{perm}}{F_{CH_4}^{0}} \tag{4.31}$$

Also, partial pressure of each species was calculated as the input for the reaction rate calculation:

$$P_{CH_4} = \left(1 - X_{CH_4}\right) \times \sigma \tag{4.32}$$

$$P_{H_2O} = \left(m - X_{H_2O}\right) \times \sigma \tag{4.33}$$

$$P_{CO} = X_{CO} \times \sigma \tag{4.34}$$

$$P_{CO_2} = X_{CO_2} \times \sigma \tag{4.35}$$

$$P_{H_2} = X_{H_2} \times \sigma \tag{4.36}$$

$$\sigma = \frac{P}{\left(1 + m + X_{H_2} - X_{CH_4} - X_{H_2O} + X_{CO} + X_{CO_2}\right)} \tag{4.37}$$

4.2.3.1 Summary of dimensionless terms used in this work.

4.2.3.1.1 Damkohler number

$$Da = \frac{TotalCatalystWeight \times k_1^o}{F_{CH_4}^o \times \sqrt{P}} \tag{4.38}$$

4.2.3.1.2 Peclet number

$$\frac{1}{Pe} = \frac{TotalMembraneArea \times \frac{B_H^o}{\delta} \times \sqrt{P}}{F_{CH_4}^o} \tag{4.39}$$

4.2.3.2. The assumptions for calculation in this model were given below;

1. Steady state operation,
2. Plug flow behavior both in reaction and permeation zone,

3. No axial mass and energy dispersions
4. Pseudo-homogeneous catalyst bed,
5. Infinite hydrogen selectivity of the membrane,
6. Ideal gas,
7. Isobaric condition for both reaction zone and permeation zone

4.2.3.3. Mathematical model for membrane reactor

4.2.3.3.1 Mass balance equations

4.2.3.3.1.1 Retentate chamber (reaction zone)

$$\frac{dX_{CH_4}}{d\zeta} = Da \times \left(R_1 + R_3\right) \tag{4.40}$$

$$\frac{dX_{H_2O}}{d\zeta} = Da \times \left(R_1 + R_2 + 2 \cdot R_3\right) \tag{4.41}$$

$$\frac{dX_{CO}}{d\zeta} = Da \times \left(R_1 - R_2\right) \tag{4.42}$$

$$\frac{dX_{CO_2}}{d\zeta} = Da \times \left(R_2 + R_3\right) \tag{4.43}$$

$$\frac{dX_{H_2}}{d\zeta} = Da \times \left(3 \cdot R_1 + R_2 + 2 \cdot R_3\right) - \frac{1}{Pe \cdot NoMembrane} \times \sum_{k=1}^{NoMembrane} J^*_{H_2,k} \tag{4.44}$$

4.2.3.3.1.2 Permeation chamber

$$\frac{dY_{H_2,k}}{d\zeta} = \frac{1}{Pe \cdot NoMembrane} \times J^*_{H_2,k} \tag{4.45}$$

4.2.3.3.2 Energy balance

4.2.3.3.2.1 Retentate chamber

$$\frac{dT}{d\zeta}=\frac{\frac{2\times\pi\times L}{F_{CH_4}^{o}}\times\left[R_{Shell}\times U\times\left(T_{wall}-T\right)-R_{Tube}\times\sum_{k=1}^{NoMembrane}U_{m,k}\times\left(T-T_k^{perm}\right)\right]+Da\times\sum_{j=1}^{3}\left(R_j\left(-\Delta H_j\right)\right)}{\left(\sum_{i=1}^{5}Cp_i\aleph_i\right)} \tag{4.46}$$

When

$$\aleph_1=\left(1-X_{CH_4}\right) \tag{4.47}$$

$$\aleph_2=\left(m-X_{H_2O}\right) \tag{4.48}$$

$$\aleph_3=X_{CO} \tag{4.49}$$

$$\aleph_4=X_{CO_2} \tag{4.50}$$

$$\aleph_5=X_{H_2} \tag{4.51}$$

4.2.3.3.2.2 Permeation chamber

$$\frac{dT_k^{perm}}{d\zeta}=\frac{\frac{2\times\pi\times R_{Tube}\times L\times U_{m,k}}{F_{CH_4}^{o}}\cdot\left(T-T_k^{perm}\right)+\frac{1}{Pe\cdot NoMembrane}J_{H_2,k}^{*}\left[h_{H_2}(T)-h_{H_2}(T_k^{perm})\right]}{Cp_{H_2}Y_{H_2}} \tag{4.52}$$

CHAPTER V

RESULTS AND DISCUSSION

5.1 Model validation

In order to verify the accuracy of mathematical model which has been used in this work, the comparison between the results from the simulation and the experimental results of Gallucci et al. [40] was performed as shown in Figure 5.1. R-square calculated from the fitting between the simulation and experimental results were equal to 0.91 and 0.97 for the conventional and membrane reactors, respectively. The results from Figure 5.1 indicated that the simulation results for both the conventional reactor and membrane reactor matched well with the experimental results.

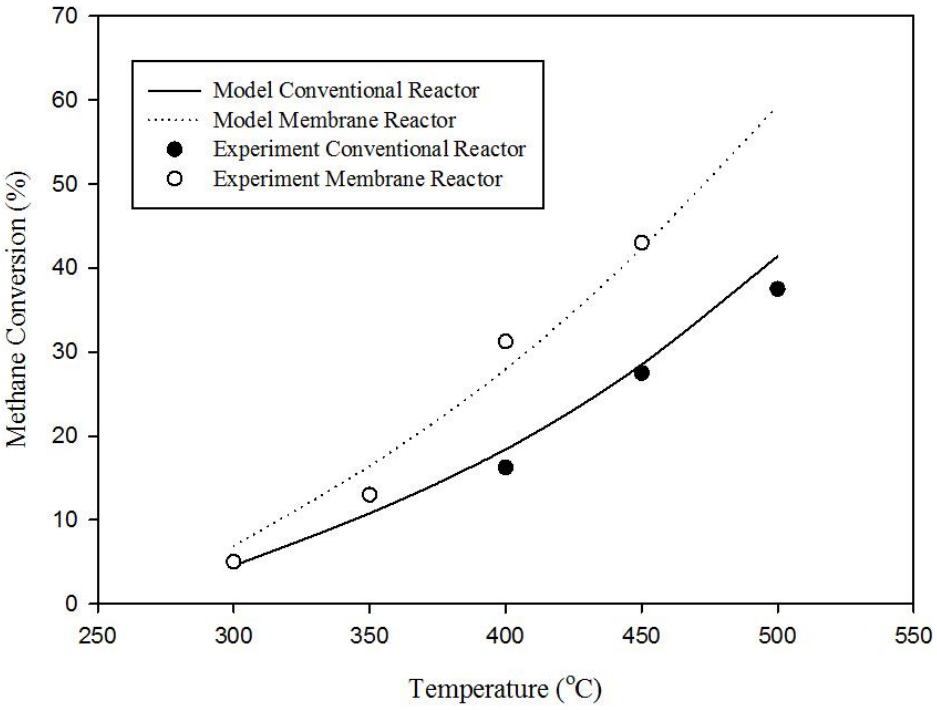

Figure 5.1 Verification of simulation model of membrane reactor between experimental and simulation results

5.2 The conventional fixed-bed and membrane reactors

In order to study the performance improvement methodology for the membrane reactor, it was necessary to well understand all working mechanisms inside the reactor and also the key operating parameters which strongly affected the reactor performance. Process modeling was the theoretical tool that could be used to demonstrate the phenomena inside the membrane reactor and visualize the effect of each operating parameters on the reactor performance. In this study, the process simulation was performed so as to identify the combined behavior of chemical reaction and membrane permeation taking place inside the membrane reactor. Effect of partial pressure of each gas components and reactor temperature on these behaviors was investigated. The dimension of membrane reactor used in this work was given in Table 5.1, while the operating conditions were given in Table 5.2. The value of log(*Da*) and log(*Pe*) of membrane reactor were determined at 4.489 and -3.699, respectively.

Table 5.1 Reactor dimensions

Parameters	Values	Units
Outside diameter	9	cm
Membrane tube diameter	1.2	cm
Void fraction	0.5	-
Reactor length	50	cm

Table 5.2 Operating condition used in the simulation of membrane reactor

Parameters	Values	Units
Methane feed flow rate	150	Mol/h
Steam to carbon ratio	3	-
Initial temperature	953	K
Pressure in reaction side	100	kPa
Pressure in permeation side	0	kPa

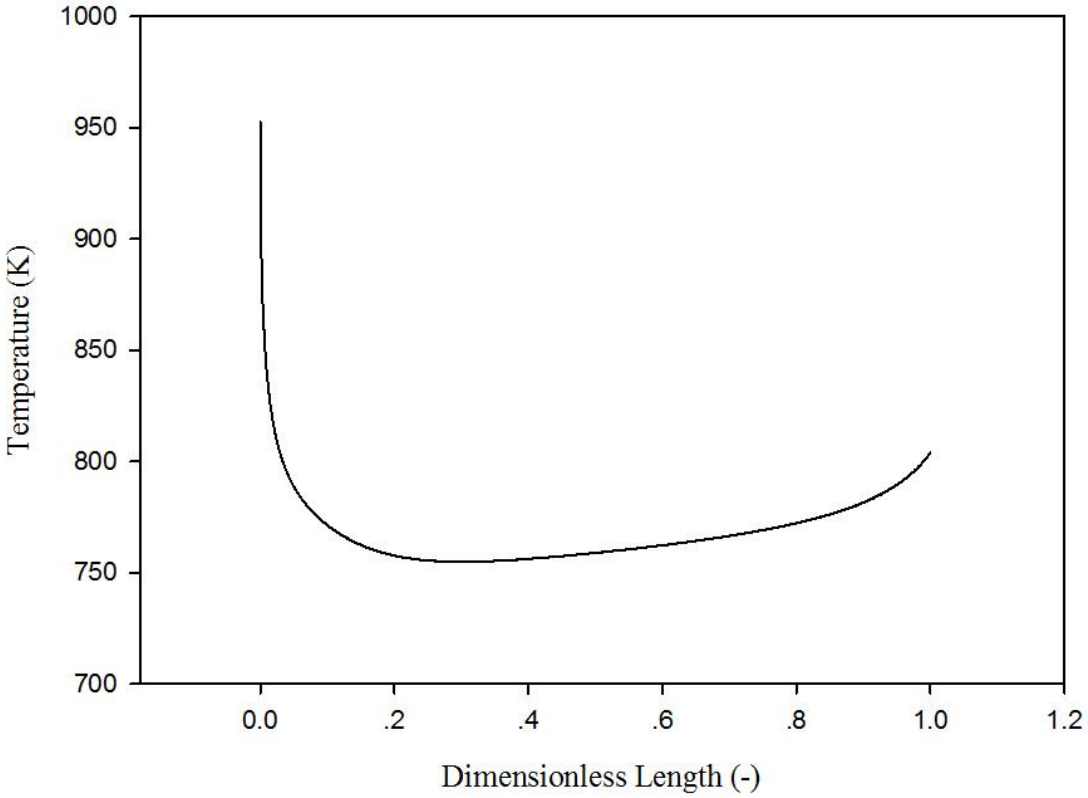

Figure 5.2 Temperature profile of uniform catalyst packing membrane reactor

Temperature profile along the length of membrane reactor was the first parameter investigated in this study due to its strong effect on both chemical reaction and H_2 permeation. As shown in Figure 5.2 in which the temperature profile at the retentate section was given, temperature extremely decreased near the reactor entrance since endothermic steam methane reforming reaction was dominated at this position. Near the center of the membrane reactor, temperature slightly increased along the reactor length because the endothermic reaction rate became lower compared to the reactor entrance, and transferred heat from heater around the reactor overcame the effect from heat of reaction. This operation recipe could be the unsafe operation since the generation of the cold spot near the reactor entrance caused the cracking of the reactor wall or membrane. These reasons inspired this research to find out the methodology to maximize the performance the membrane reactor under thermal-safe operation.

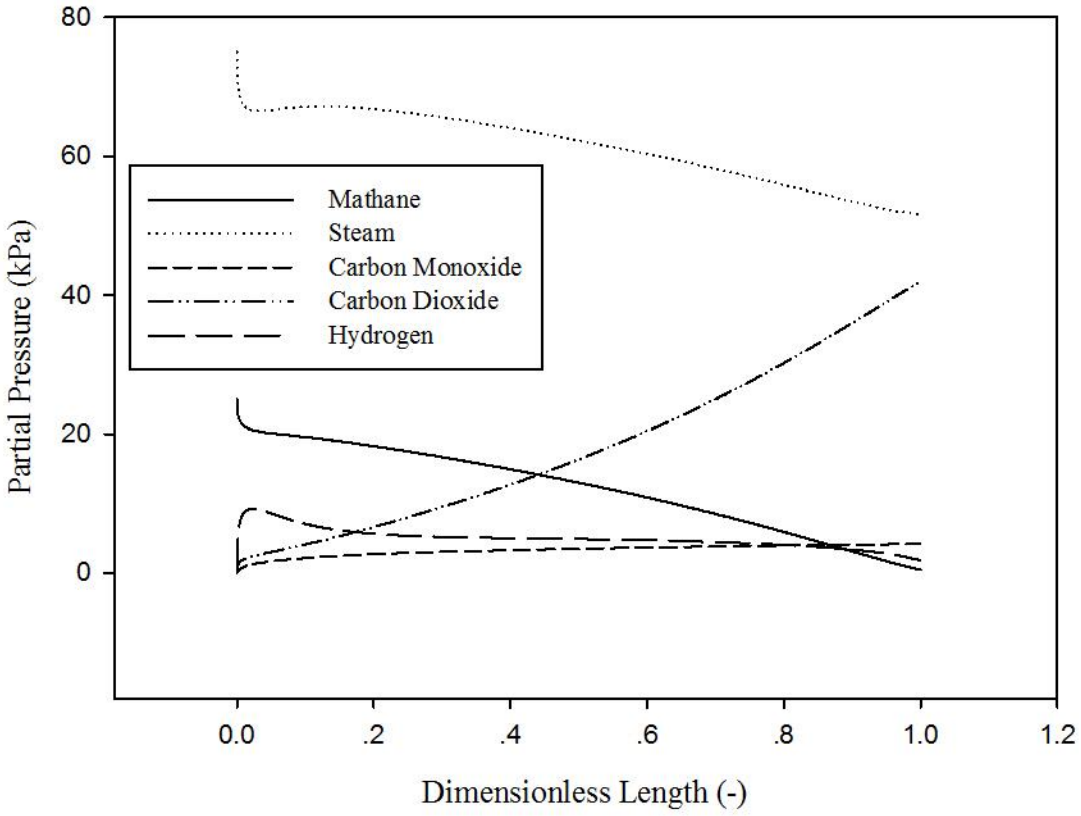

Figure 5.3 Distribution of partial pressure of each gas component along the reactor length for uniform catalyst packing membrane reactor

The partial pressure of each component was also important process parameters for the operation of membrane reactor due to its highly influence on reaction rate and H_2 permeation rate similar to temperature. The partial pressure distribution along the reactor of each gas component was illustrated in Figure 5.3. In this figure, for methane and steam which were the reactants for steam methane reforming reaction, their partial pressure extremely decreased in the starting path because of high reaction rate and moderately decreased thereafter due to lower reaction rate. Inversely, for carbon monoxide and carbon dioxide, the products from steam methane reforming and water gas shift reactions, their partial pressure increased along the reactor. However, the carbon monoxide partial pressure at the exit of reactor was lower than carbon dioxide partial pressure owing to the participation of water gas shift reaction. Also, partial pressure of hydrogen extremely increased near the reactor entrance; however it decreased afterward since H_2 generated at

the retentate (reaction) chamber permeated through the membrane to the permeation section due to the difference of H_2 partial pressure of each section of membrane reactor.

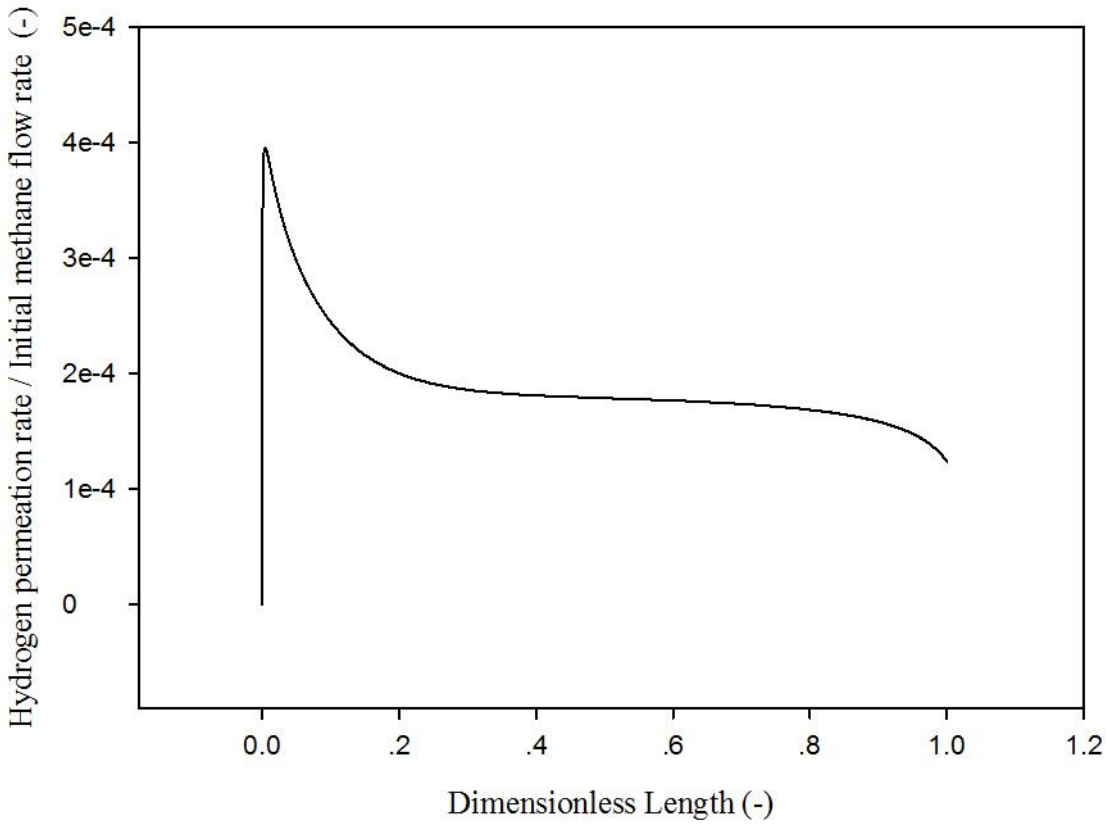

Figure 5.4 Distribution of hydrogen permeation rate along the reactor length for uniform catalyst packing membrane reactor

The permeation rate of hydrogen through membrane plays an important role in controlling H_2 yield of the membrane reactor. Pure H_2 was obtained at the permeation section of membrane reactor because Pd-based membrane allowed only hydrogen to permeate through. The distribution of permeation rate of hydrogen to initial methane flow rate along the reactor length was shown in Figure 5.4. This figure showed that the hydrogen permeation rate was high near the reactor entrance; however, the permeation rate decreased with the reactor length thereafter due to lower in the H_2 partial pressure difference between retentate chamber and permeation chamber which was the driving force for the permeation of H_2.

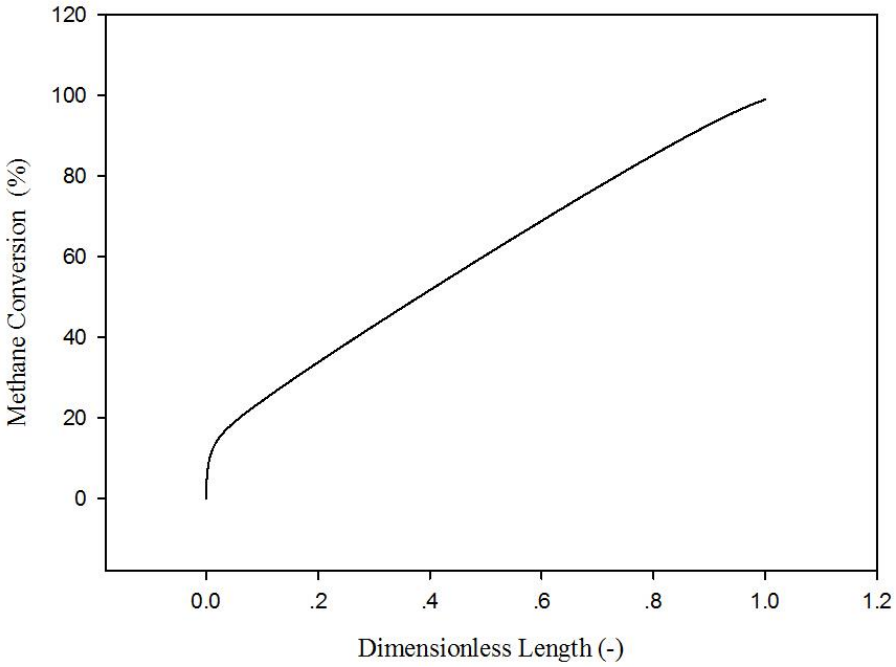

Figure 5.5 Distribution of the methane conversion along the reactor length for uniform catalyst packing membrane reactor

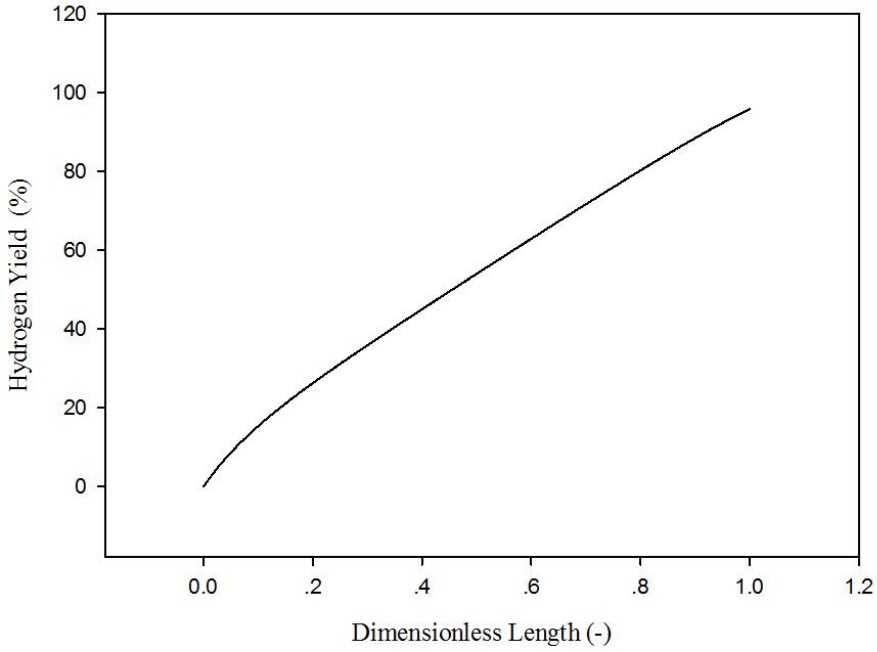

Figure 5.6 Distribution of hydrogen yield along the reactor length for uniform catalyst packing membrane reactor

The methane conversion and hydrogen yield distributions along the reactor length of membrane reactor were shown in Figures 5.5 and 5.6, respectively. Both methane conversion and hydrogen yield increased along the reactor length; however, the increasing rate of methane conversion near the reactor entrance was extremely higher than that of hydrogen yield because the rate of steam methane reforming reaction taking place at the retentate chamber was far higher than H_2 permeation rate at this position. The reason was that H_2 partial pressure at the retentate chamber near the reactor entrance was quite small causing low driving force of H_2 permeation at this position. Subsequently, the increasing rate of methane conversion and hydrogen yield became constant along the membrane reactor.

5.3 The correlation of the Da and Pe of conventional membrane reactor

Kikuchi [41] suggested that hydrogen permeation rate should be well related with hydrogen formation rate in retentate chamber to achieve high performance of membrane reactor. According to Dixon [42], three operating parameters of membrane reactor, i.e. the reaction rate, H_2 permeation rate and reactant feed rate strongly related to one another. The Damkohler number (*Da*) and Peclet number (*Pe*) are the dimensionless numbers used to explain the correlation between maximum reaction rate and maximum convection rate, and between maximum permeation rate and maximum convection rate, respectively. These two numbers were key dimensionless parameters used to design membrane reactor and evaluate its performance.

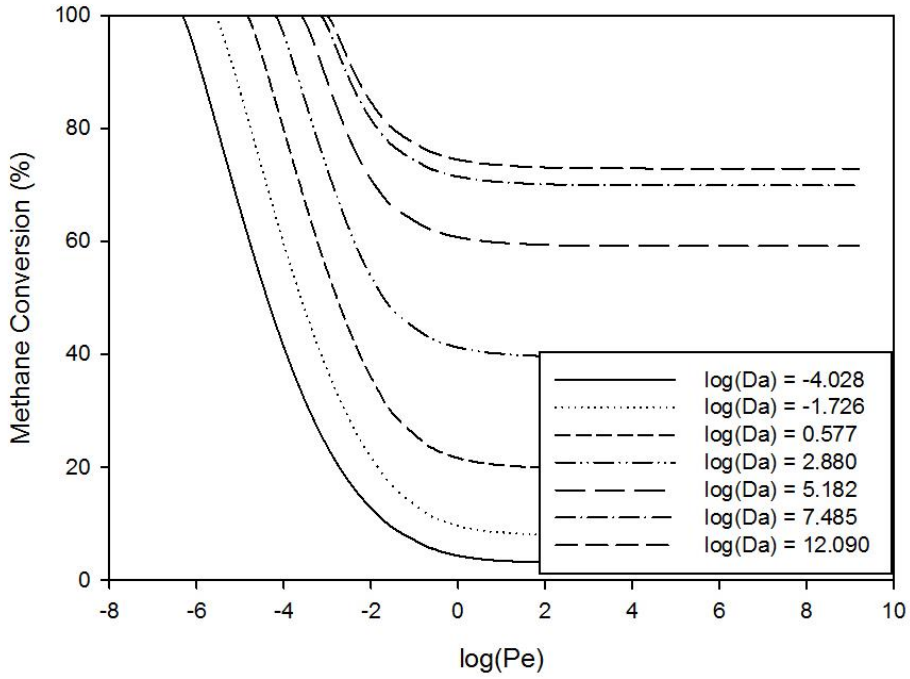

Figure 5.7 Relationship between methane conversion and Peclet number at different Damkohler number

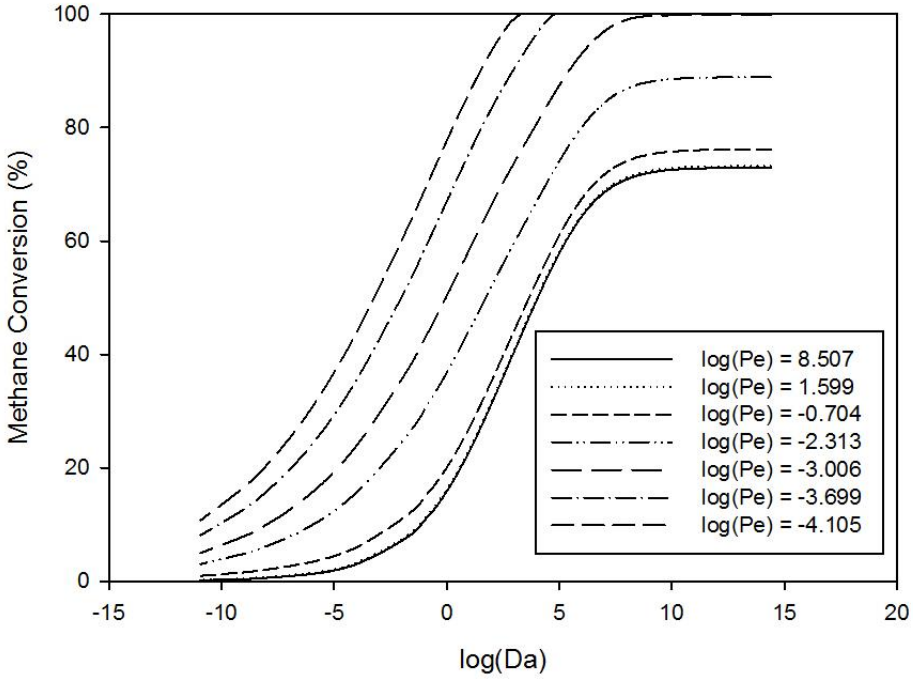

Figure 5.8 Relationship between methane conversion and Damkohler number at different Peclet number

The methane conversion at the reactor exit at different Peclet number and Damkohler number was shown in Figures 5.7 and 5.8. These results indicated that methane conversion increased as Damkohler number increased at constant Peclet number. Inversely, methane conversion increased as Peclet number decreased for constant Damkohler number. Operating at high Peclet number (> 0), the methane conversion did not change as Peclet number increased because the membrane permeability became very low and membrane could not properly work in the reaction rate acceleration. The reason above caused the performance membrane reactor operating at high Peclet number offered to be almost identical to the conventional reactor. For the operation at low Damkohler number (< -10), methane conversion was almost zero. For the operation at high Damkohler number, methane conversion strongly depended on Peclet number because the reaction rate became faster compared to H_2 permeation rate.

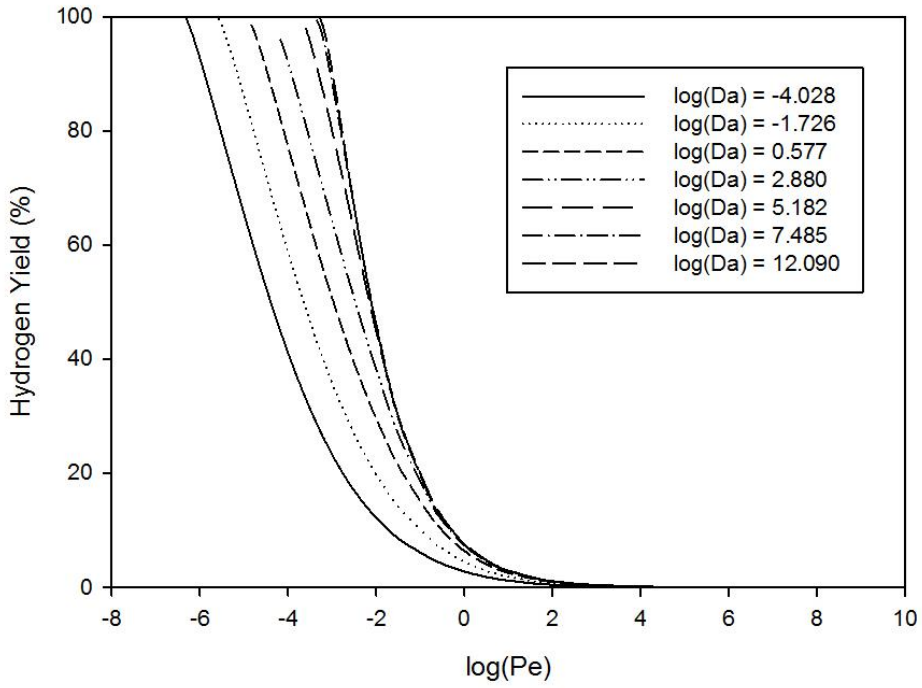

Figure 5.9 Relationship between H_2 yield and Damkohler number at different Peclet number

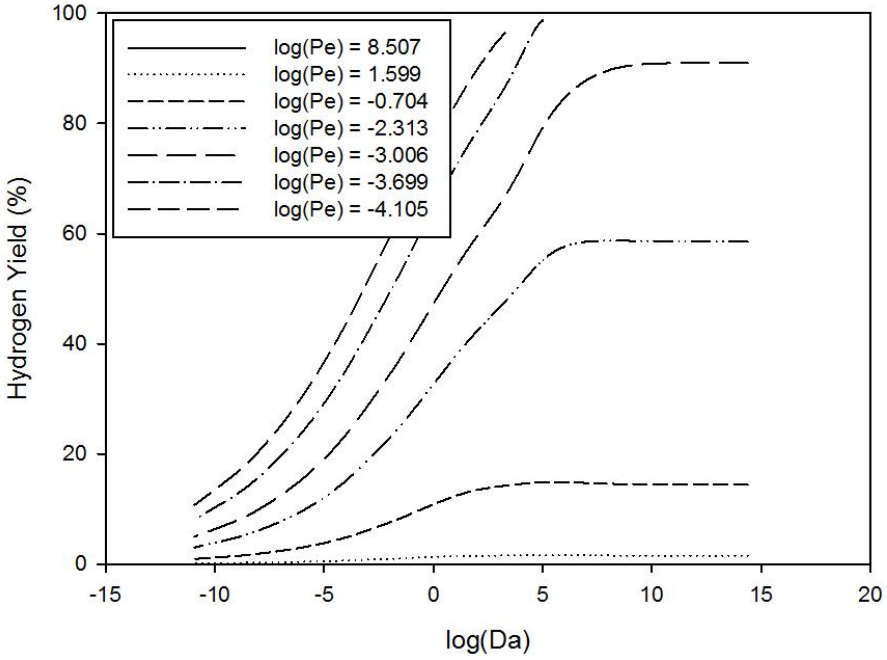

Figure 5.10 Relationship between H_2 yield and Peclet number at different Damkohler number

The relationships between hydrogen yield at the reactor exit of membrane reactor with Peclet number and Damkohler Number were shown in Figures 5.9 and 5.10. The results demonstrated that the hydrogen yield increased with Damkohler number for constant Peclet number, while the hydrogen yield increased as Peclet number decreased for constant Damkohler number. Operating at high Peclet number, the behavior membrane reactor was almost similar to that of conventional reactor at any Damkohler number. Therefore, the hydrogen yield of membrane reactor was nearly equal to zero. Operating at high Damkohler number, the membrane reactor reached hydrogen permeation limitation and the hydrogen yield therefore solely depended on Peclet number.

5.4 Non-uniform membrane area and catalyst distribution for membrane reactor

For the non-uniform membrane reactor, the reactor was divided into two sections with different catalyst packing density and amount of membrane area. However, the total

catalyst weight and amount of membrane area were determined to be similar for all scenarios in this study.

To make easier understanding, the abbreviation used in this work was Φ_{CAT} = A, Φ_{MEM} = B. Φ_{CAT} stood for the catalyst fraction of the first section of reactor, while the value of catalyst fraction of the first section was given instead of "A". Φ_{MEM} stood for the membrane area fraction of the first section as its value was given instead of "B". For example, Φ_{CAT} = 0.5, Φ_{MEM} = 0.2 represented the membrane reactor with the catalyst fraction of 0.5 at the 1st section and the membrane area of 0.2 at the 1st section. The operating temperature, total pressure of reaction side and steam to carbon ratio were determined at 953 K, 100 kPa and 3, respectively. Vacuum operation was used in the permeation side to conduct hydrogen permeation through membrane. The log(*Da*) and log(*Pe*) of membrane reactor were set to be equal to 4.489 and -3.699, respectively.

Reaction temperature was judged to be critical parameter due to its influence on both reaction rate and permeation rate of membrane reactor. The temperature profiles of non-uniform distribution of membrane allocation and catalyst density were shown in Figure 5.11. In this figure, Φ_{CAT} = 0.5, Φ_{MEM} = 0.5 represented uniform distribution membrane reactor. Φ_{CAT} = 0.5, Φ_{MEM} = 0.2 and Φ_{CAT} = 0.5, Φ_{MEM} = 0.8 were non-uniform distribution membrane reactor with the variation of membrane allocation. Φ_{CAT} = 0.2, Φ_{MEM} = 0.5 and Φ_{CAT} = 0.8, Φ_{MEM} = 0.5 were non-uniform distribution membrane reactor with the variation of catalyst density.

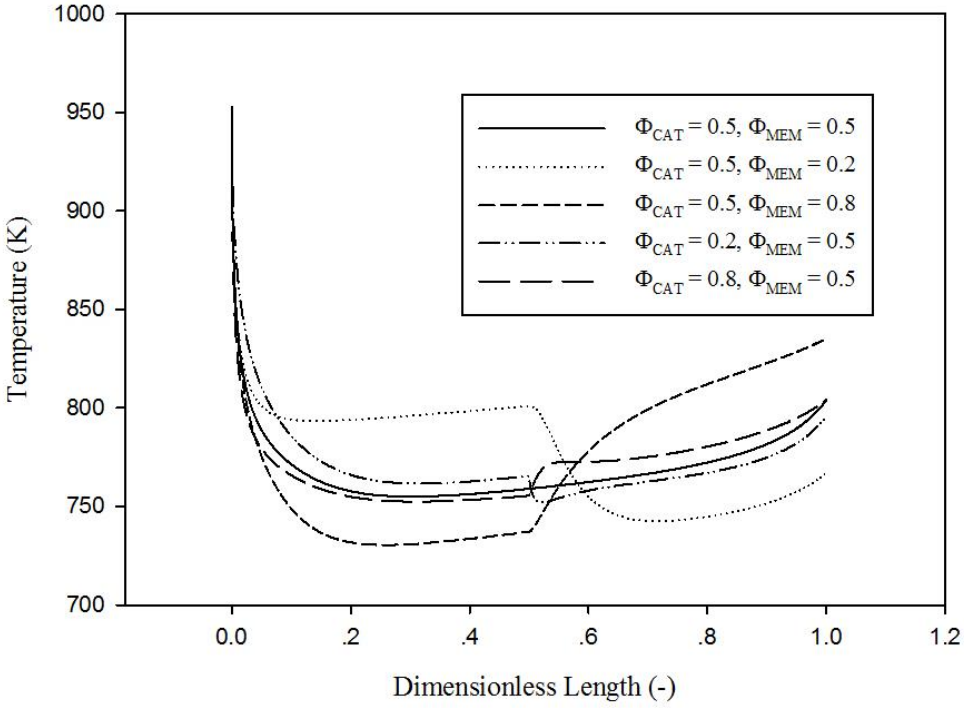

Figure 5.11 Distribution of temperature along the reactor length of uniform distribution and non-uniform distribution membrane reactors

For Φ_{CAT} = 0.2, Φ_{MEM} = 0.5, its temperature in the first section was higher than that of uniform distribution membrane reactor because of lower reaction rate. Nevertheless, in the second section, the inverse trend in temperature was found. In case of Φ_{CAT} = 0.8, Φ_{MEM} = 0.5, the trend in temperature was opposite to that observed in Φ_{CAT} = 0.2, Φ_{MEM} = 0.5. For the membrane reactor with Φ_{CAT} = 0.5, Φ_{MEM} = 0.2 configuration, the temperature at the first section was higher than uniform distribution case due to its lower endothermic steam methane reforming reaction rate and also H_2 permeation rate. However, the temperature at the second section was lower than at the first section because of its higher steam reforming reaction rate induced by high H_2 permeation rate. In case of Φ_{CAT} = 0.5, Φ_{MEM} = 0.8, the temperature trend was opposite to that observed in Φ_{CAT} = 0.5, Φ_{MEM} = 0.2.

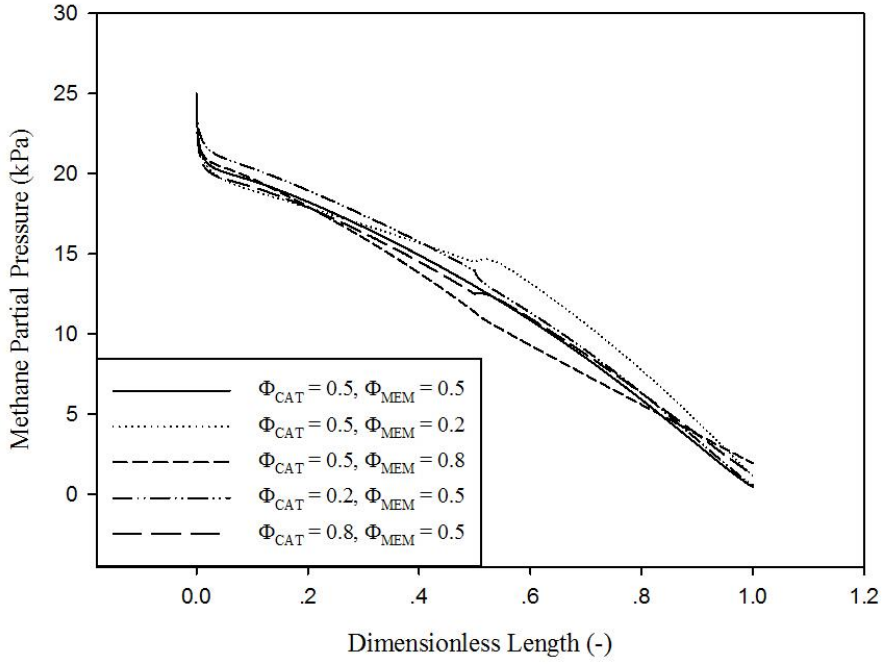

Figure 5.12 Distribution of methane partial pressure along the reactor length of uniform distribution and non-uniform distribution membrane reactors

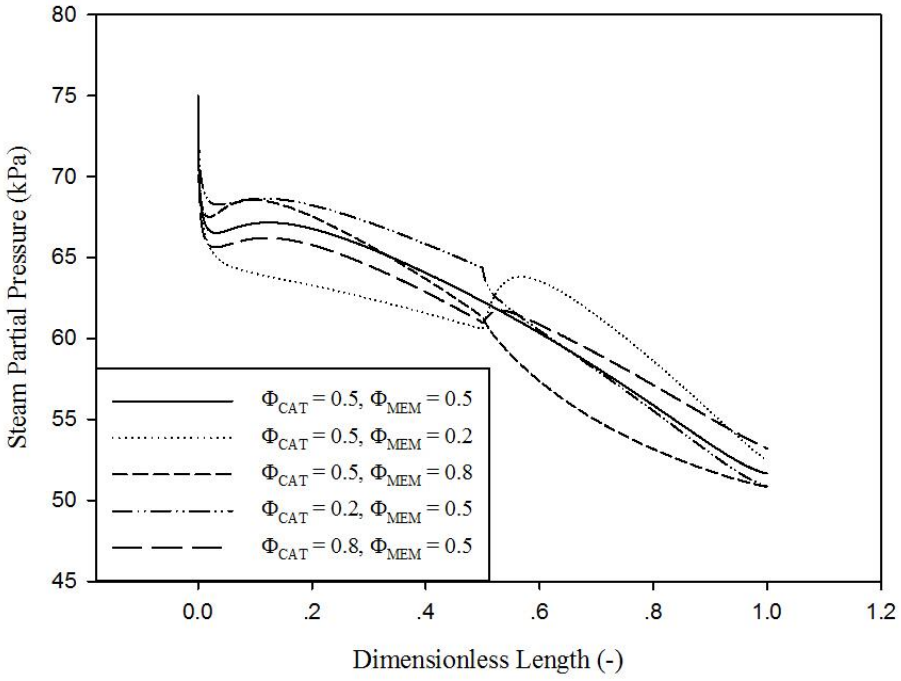

Figure 5.13 Distribution of steam partial pressure along the reactor length of uniform distribution and non-uniform distribution membrane reactors

The partial pressure of each gas reactant also played an important role in controlling chemical reaction rate inside the membrane reactor. The profiles of partial pressure of methane and steam, which were the reactant for steam methane reforming reaction, were illustrated in Figures 5.12 and 5.13, respectively. These results showed that the partial pressure of reactant observed in Φ_{CAT} = 0.5, Φ_{MEM} = 0.2 was lower than the uniform distribution membrane reactor in the first section because of higher partial pressure of H_2 product. Lower membrane area at the first section caused lower H_2 permeation; hence, most of hydrogen generated in the retentate side could not permeate to the permeation side. However, in the second section, the opposite trend in reactant partial pressure to the first section was observed. For Φ_{CAT} = 0.2, Φ_{MEM} = 0.5, its partial pressure of reactant was higher than uniform distribution in the first section because of lower reaction rate of the former. Conclusively, the trends in reactant partial pressure observed in Φ_{CAT} = 0.8, Φ_{MEM} = 0.5 and Φ_{CAT} = 0.5, Φ_{MEM} = 0.8 was opposite to those observed in Φ_{CAT} = 0.2, Φ_{MEM} = 0.5 and Φ_{CAT} = 0.5, Φ_{MEM} = 0.2.

High hydrogen partial pressure in the retentate side was expected in order to enhance the hydrogen permeation rate and also hydrogen yield of membrane reactor. Figure 5.14 showed the partial pressure of hydrogen inside the uniform distribution and non-uniform distribution membrane reactor. In this figure, the membrane reactor with Φ_{CAT} = 0.2, Φ_{MEM} = 0.5 configuration offered lower hydrogen partial pressure at the first section than uniform distribution membrane reactor because of lower reaction rate. However, H_2 partial pressure of Φ_{CAT} = 0.2, Φ_{MEM} = 0.5 became higher than that of uniform distribution membrane reactor at the second section. For Φ_{CAT} = 0.8, Φ_{MEM} = 0.5, its trend in hydrogen partial pressure profile was opposite to Φ_{CAT} = 0.2, Φ_{MEM} = 0.5. In case of Φ_{CAT} = 0.5, Φ_{MEM} = 0.2, the partial pressure of hydrogen in the first section was higher than uniform distribution membrane reactor due to lower membrane permeability of the former, while hydrogen partial pressure of the former became lower than uniform distribution membrane reactor at the 2nd section. Also, the opposite trend in H_2 partial pressure was found for Φ_{CAT} = 0.5, Φ_{MEM} = 0.8 compared to Φ_{CAT} = 0.5, Φ_{MEM} = 0.2.

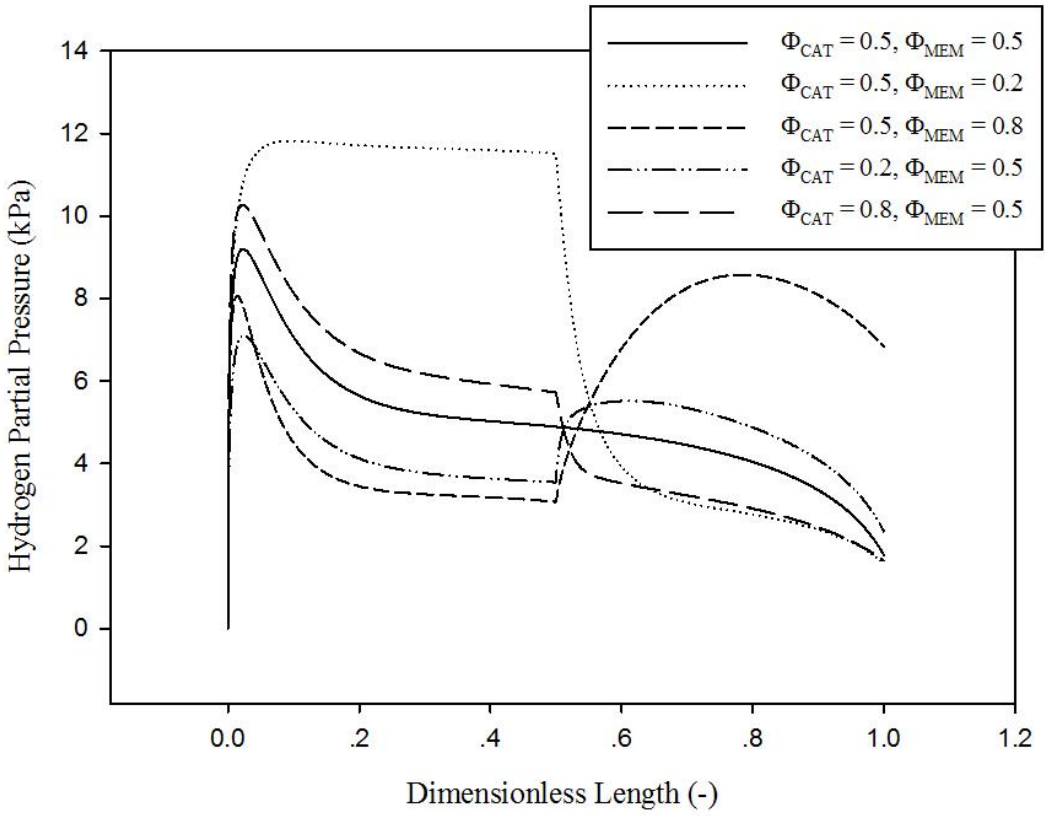

Figure 5.14 Distribution of hydrogen partial pressure along the reactor length of uniform distribution and non-uniform distribution membrane reactors

The methane conversion profiles of non-uniform distribution and uniform distribution membrane reactors were illustrated in Figure 5.15. This results showed that methane conversion of Φ_{CAT} = 0.5, Φ_{MEM} = 0.2 was lower than that of uniform distribution membrane reactor at the first section; however, methane conversion became higher at the 2nd section. This implied that higher membrane area could offer H_2 permeation rate and the steam methane reforming reaction was then shifted forward. Similar relationship between membrane area and methane conversion was also observed in the membrane reactor with Φ_{CAT} = 0.5, Φ_{MEM} = 0.8 configuration. For Φ_{CAT} = 0.2, Φ_{MEM} = 0.5, because its catalyst weight in the first section was lower than uniform distribution membrane reactor, the lower reaction rate and also methane conversion was obtained. It could be concluded that the methane conversion could be improved as membrane reactor was equipped with large membrane area and also high catalyst density.

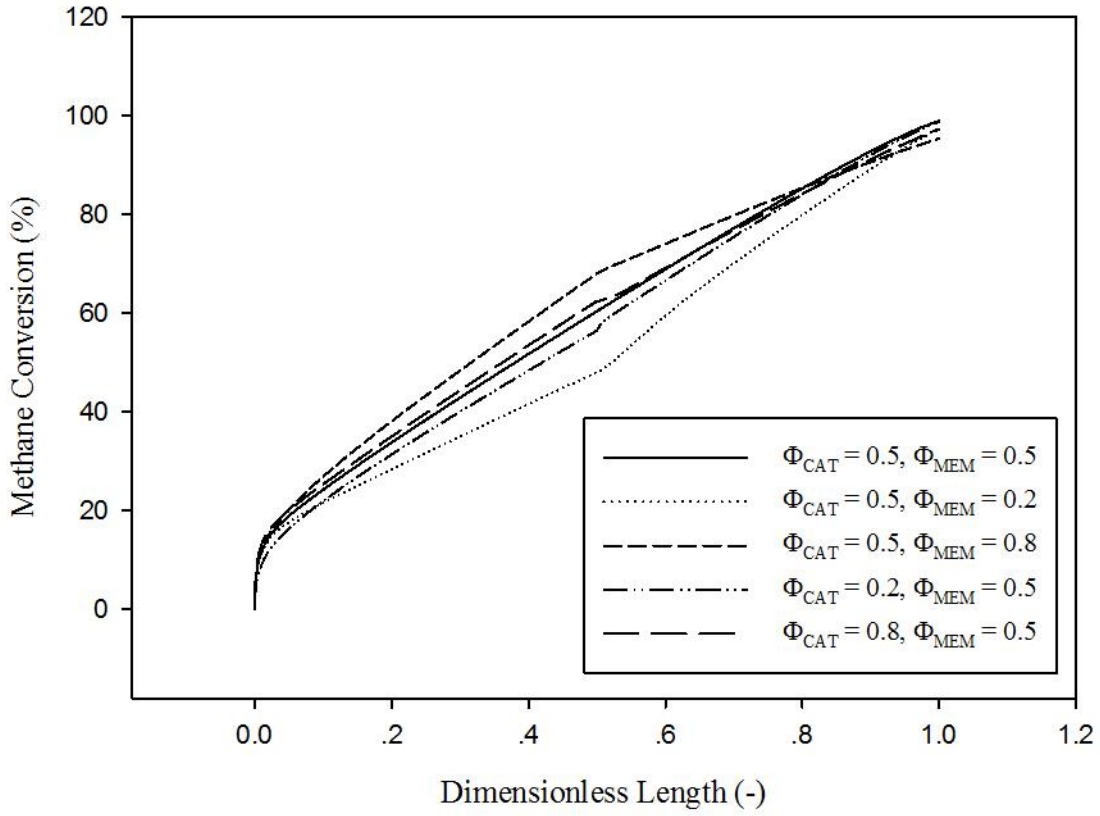

Figure 5.15 Distribution of methane conversion along the reactor length of uniform distribution and non-uniform distribution membrane reactors

The hydrogen yield profile was shown in the Figure 5.16. The results showed that the hydrogen yield at the first section of Φ_{CAT} = 0.5, Φ_{MEM} = 0.2 was lower than uniform distribution membrane reactor, but it became higher at the second section. With larger membrane area, membrane reactor could offer higher H_2 yield due to higher H_2 permeation rate. The same membrane area-H_2 yield relationship was also found in Φ_{CAT} = 0.5, Φ_{MEM} = 0.8. Considering the effect of catalyst distribution, the hydrogen yield of Φ_{CAT} = 0.2, Φ_{MEM} = 0.5 was lower than uniform distribution membrane reactor at the first section but it became higher at the second section. However, for Φ_{CAT} = 0.8, Φ_{MEM} = 0.5, its hydrogen yield was higher than uniform distribution membrane reactor at the first section. This indicated that the increase in catalyst density could promote hydrogen yield in the membrane reactor.

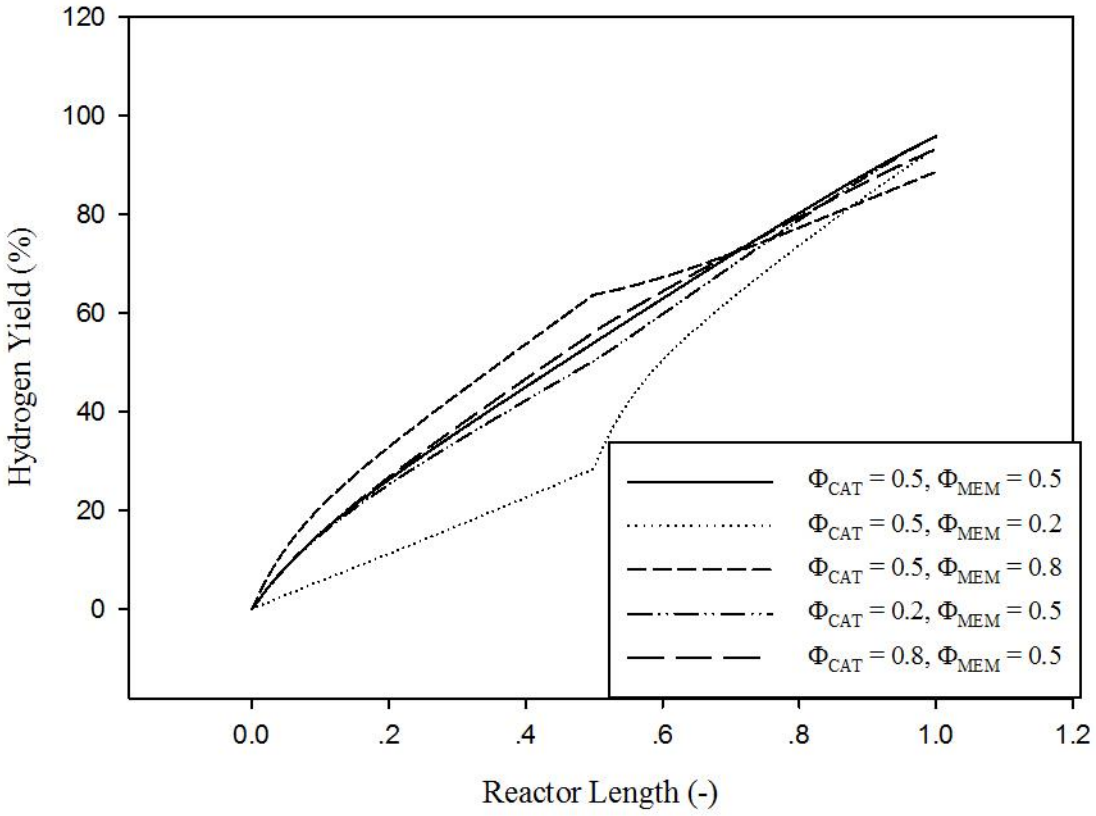

Figure 5.16 Distribution of hydrogen yield along the reactor length of uniform distribution and non-uniform membrane reactors

5.5 The performance of non-uniform distribution membrane reactor in term of Da and Pe

Although non-uniform catalyst distribution and membrane allocation could be used for increasing the performance of membrane reactor, the suitable distributions of catalyst density and membrane area should be also considered. The reaction rate, permeation rate and convection rate were very important factors controlling the performance of membrane reactor. All of these three variables were correlated to one another via two dimensionless numbers, Damkohler number (*Da*) and Peclet number (*Pe*), in order to find the optimum distributions of catalyst density and membrane area.

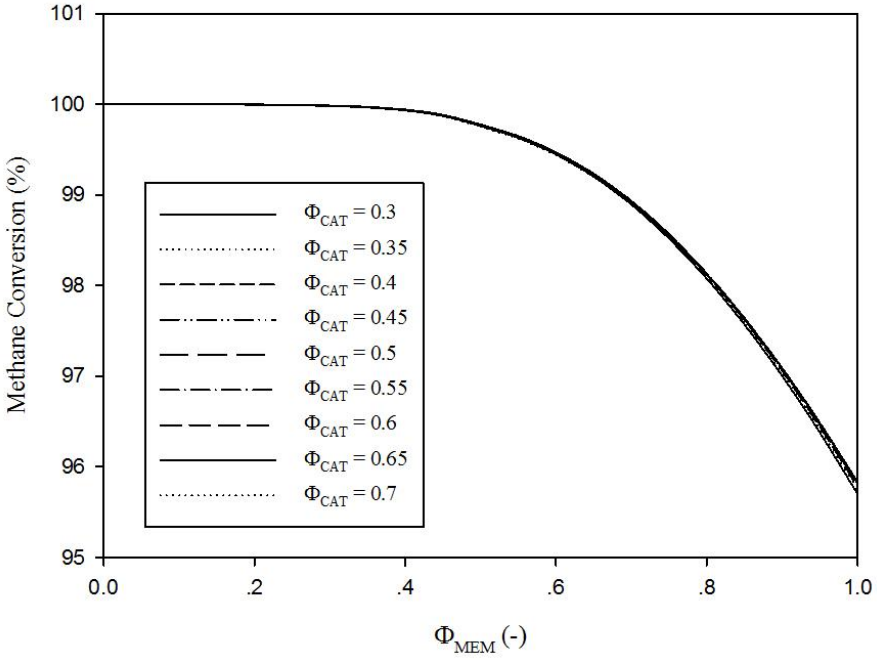

(a) log(*Da*) = 9.787, log(*Pe*) = -3.006

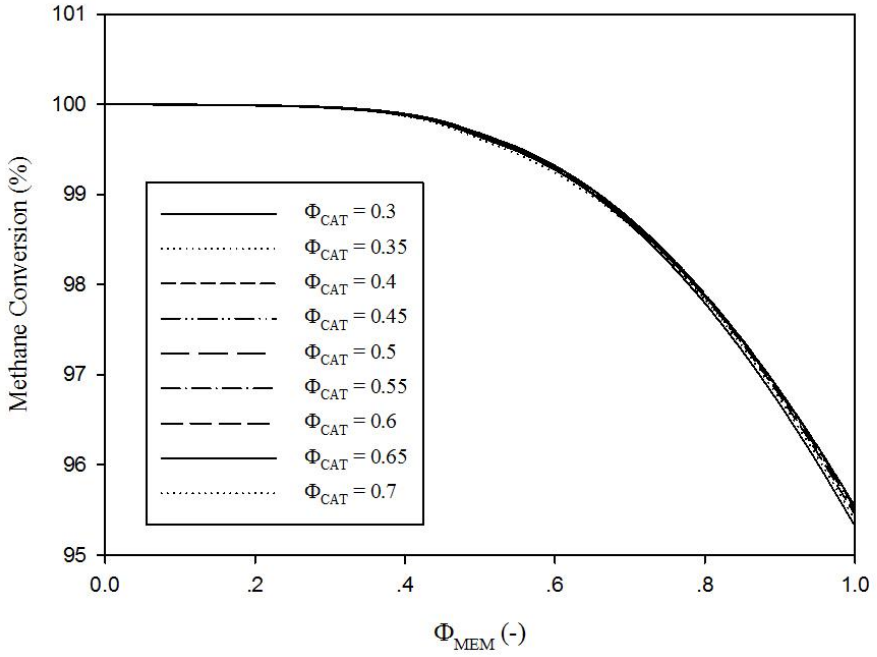

(b) log(*Da*) = 9.094, log(*Pe*) = -3.006

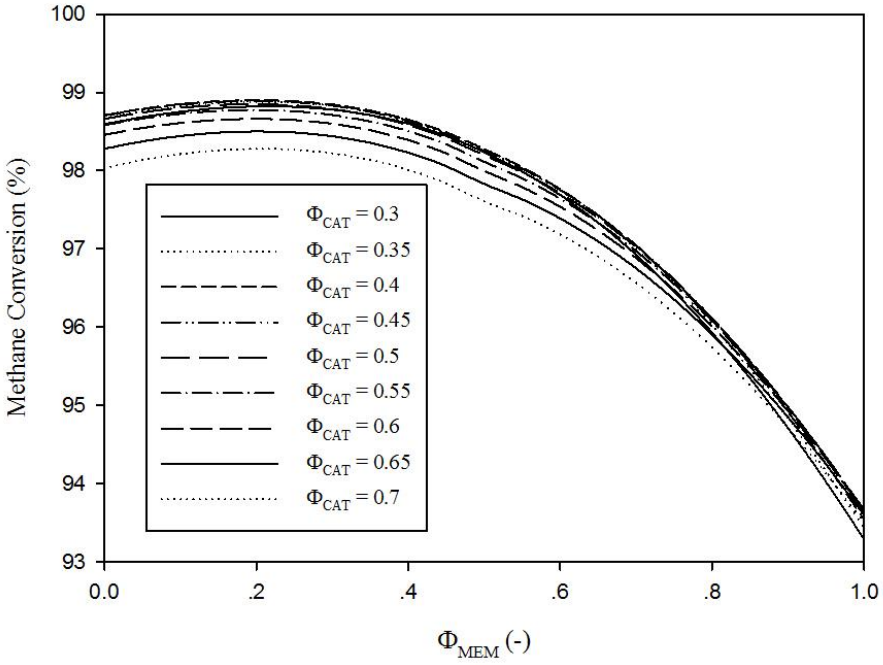

(c) log(*Da*) = 7.485, log(*Pe*) = -3.006

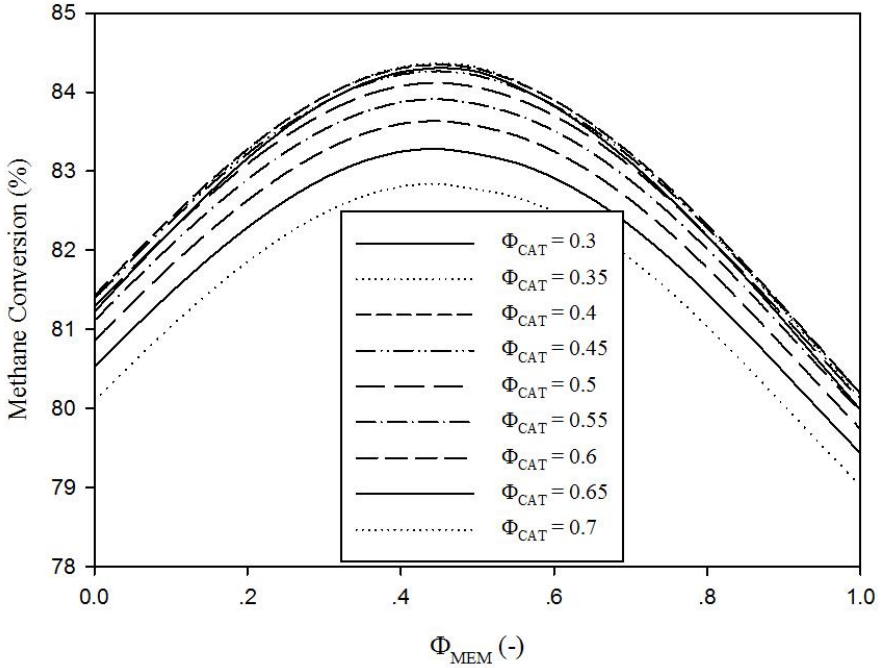

(d) log(*Da*) = 4.489, log(*Pe*) = -3.006

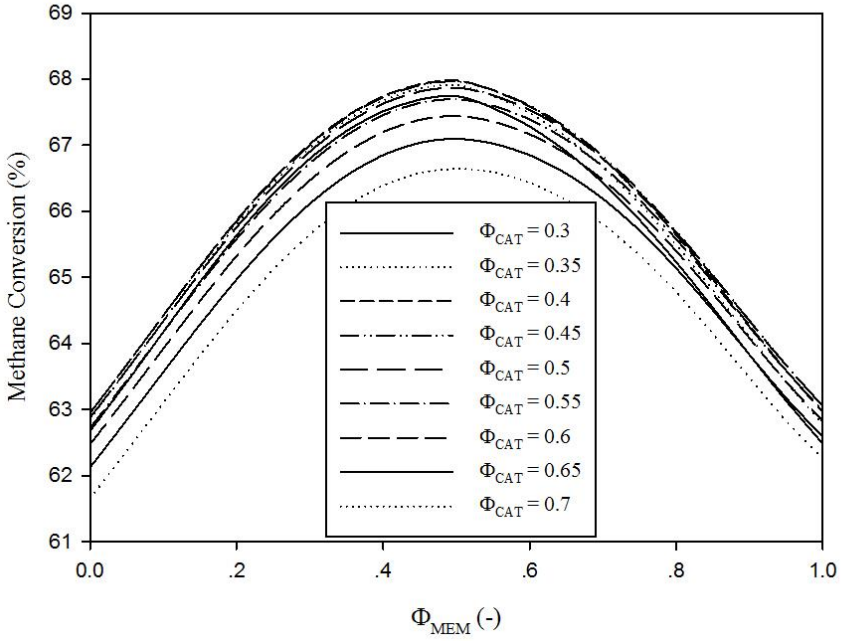

(e) log(*Da*) = 2.186, log(*Pe*) = -3.006

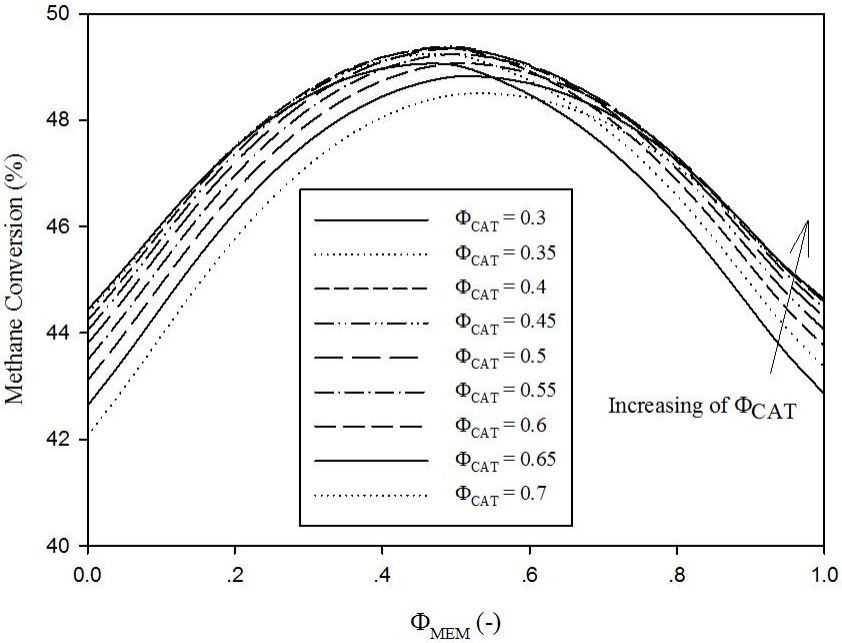

(f) log(*Da*) = -0.116, log(*Pe*) = -3.006

Figure 5.17 Methane conversion at the reactor exit of non-uniform distribution membrane reactor at different *Da* and constant *Pe*

Figure 5.17 showed methane conversion at the exit of uniform and non-uniform distribution of membrane reactors with different *Da* number. Peclet number for every scenario given in Fig. 5.17 was kept to be -3.006. When the catalyst density (*Da* number) was very high, the suitable fraction of membrane area at the 1st section, which offered maximum methane conversion, approached to 0. The adjustment of catalyst fraction of each reactor section could not significantly improve the methane conversion because of the limitation in H_2 permeation capacity.

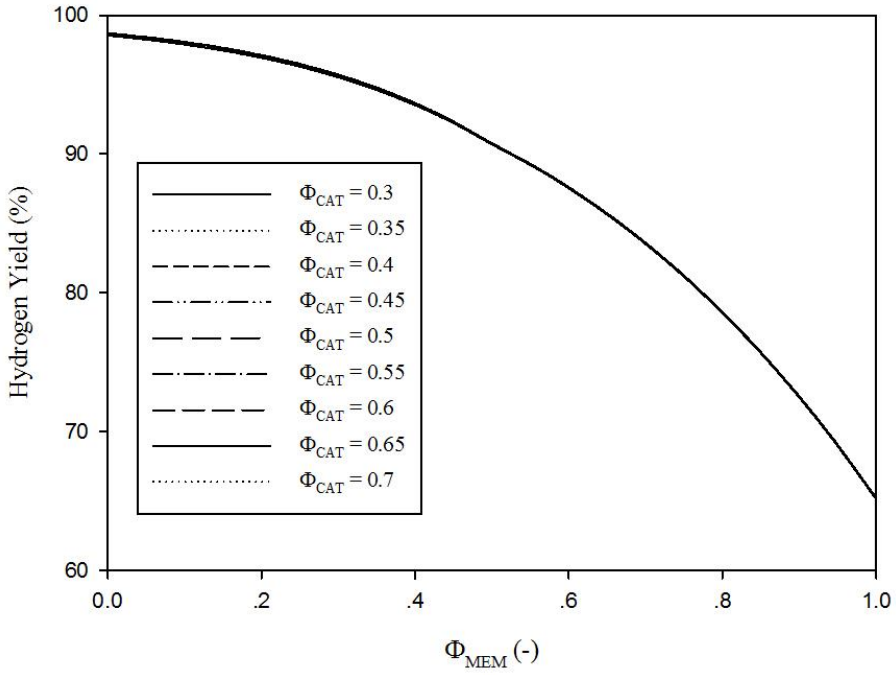

(a) log(*Da*) = 9.787, log(*Pe*) = -3.006

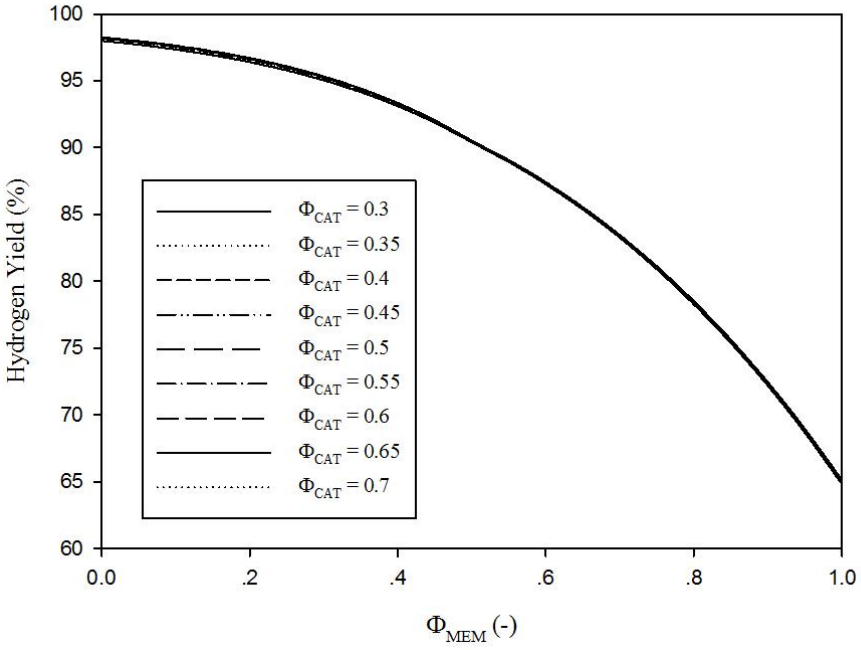

(b) log(*Da*) = 9.094, log(*Pe*) = -3.006

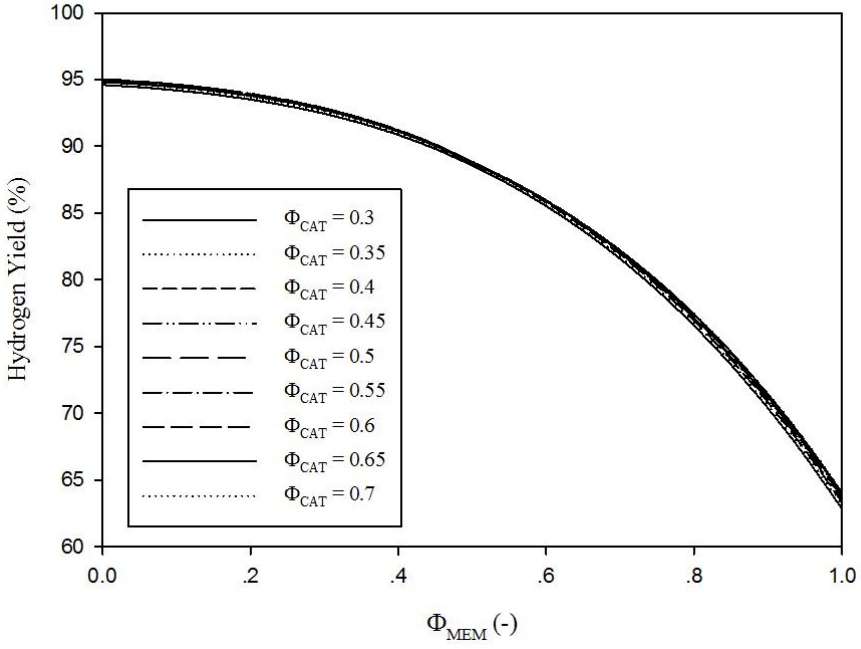

(c) log(*Da*) = 7.485, log(*Pe*) = -3.006

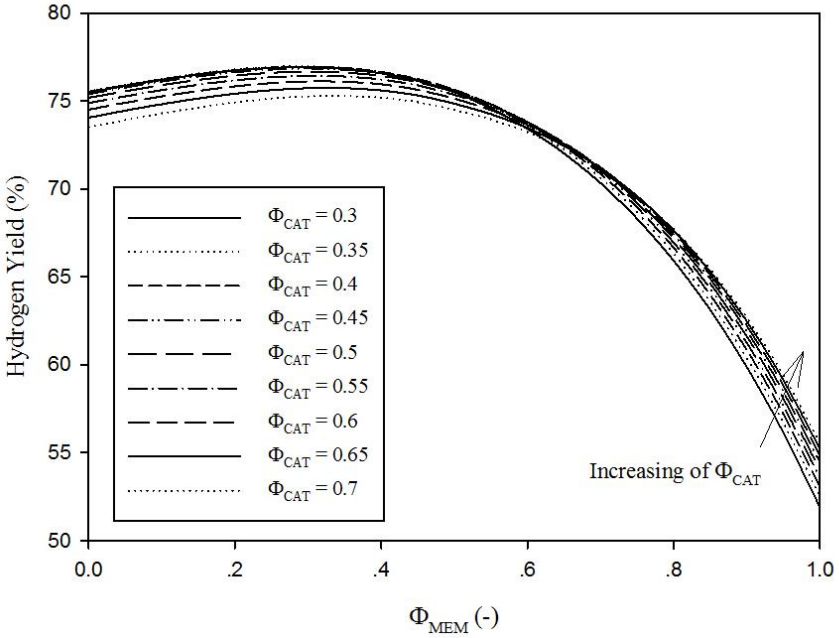

(d) log(*Da*) = 4.489, log(*Pe*) = -3.006

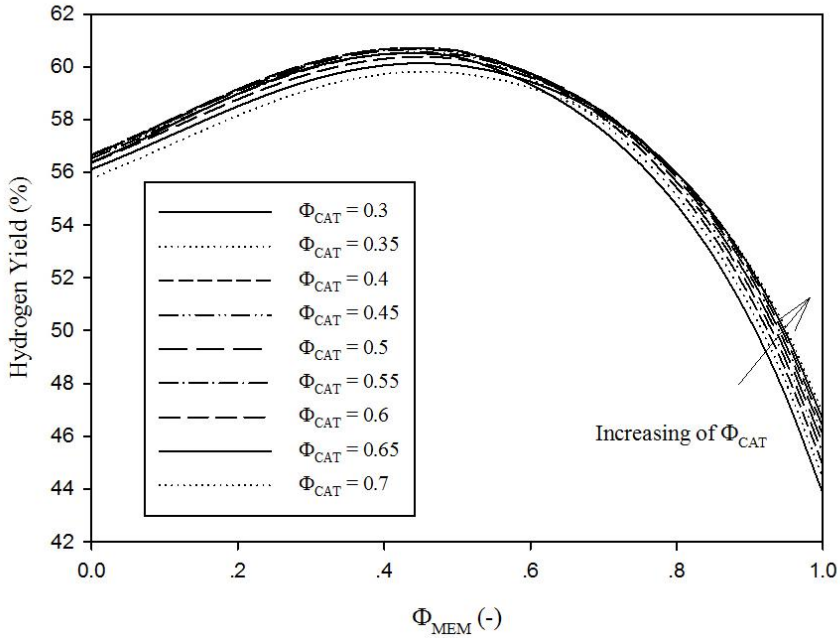

(e) log(*Da*) = 2.186, log(*Pe*) = -3.006

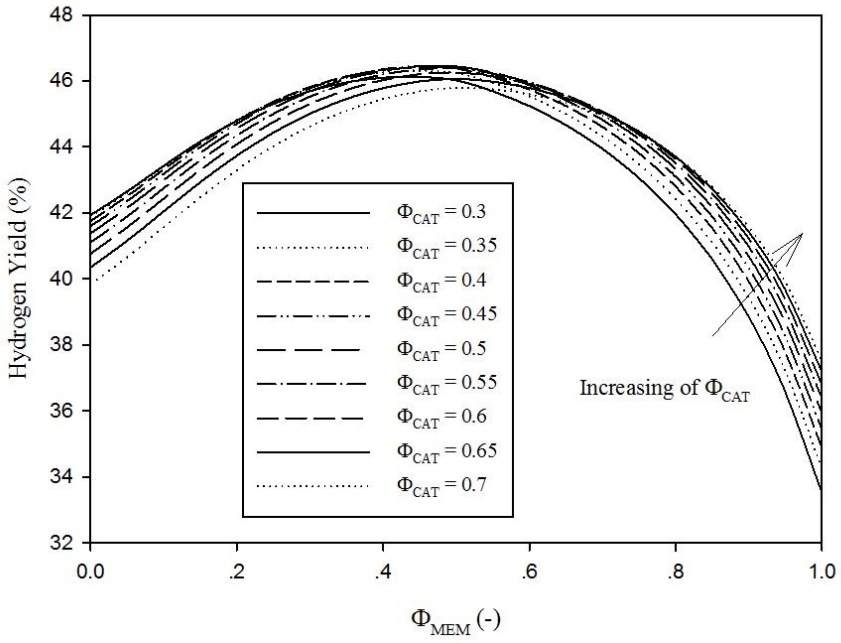

(f) log(*Da*) = -0.116, log(*Pe*) = -3.006

Figure 5.18 H_2 yield at the reactor exit of non-uniform distribution membrane reactor at different *Da* and constant *Pe*

Figure 5.18 showed hydrogen yield at the exit of non-uniform distribution and uniform distribution membrane reactors with different *Da* number. Peclet number was kept to be constant at -3.006. The results showed that, for the reactor configuration with high total catalyst density (high *Da* number), H_2 yield became its maximum value as membrane fraction at the 1st section was equal to 0. Also, the adjustment of catalyst distribution could not improve the hydrogen yield for the membrane reactor configuration with high *Da* number since H_2 permeation became the slow step which controlled overall mechanism inside the membrane reactor. As log(*Da*) = 9.787, log(*Pe*) = -3.006, the optimum catalyst and membrane fraction at the 1st reactor section that offered optimum methane conversion and H_2 yield were equal to 0.55 and 0, respectively.

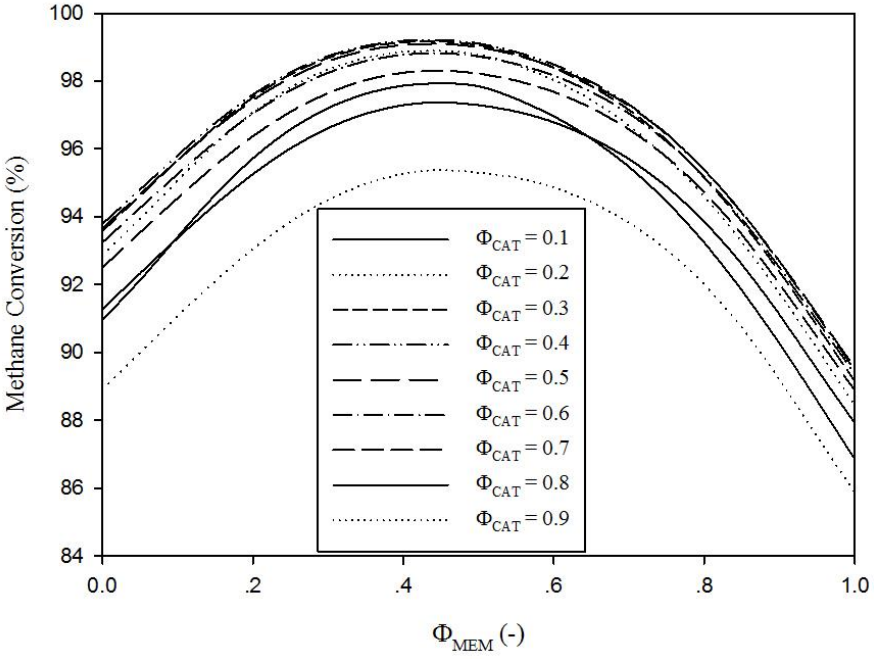

(a) log(*Da*) = 4.489, log(*Pe*) = -3.699

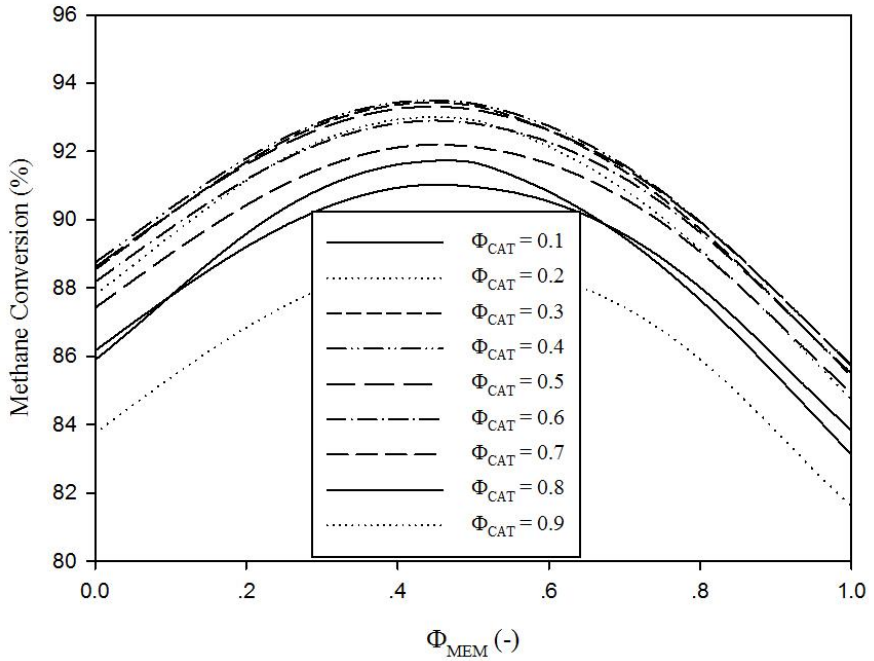

(b) log(*Da*) = 4.489, log(*Pe*) = -3.412

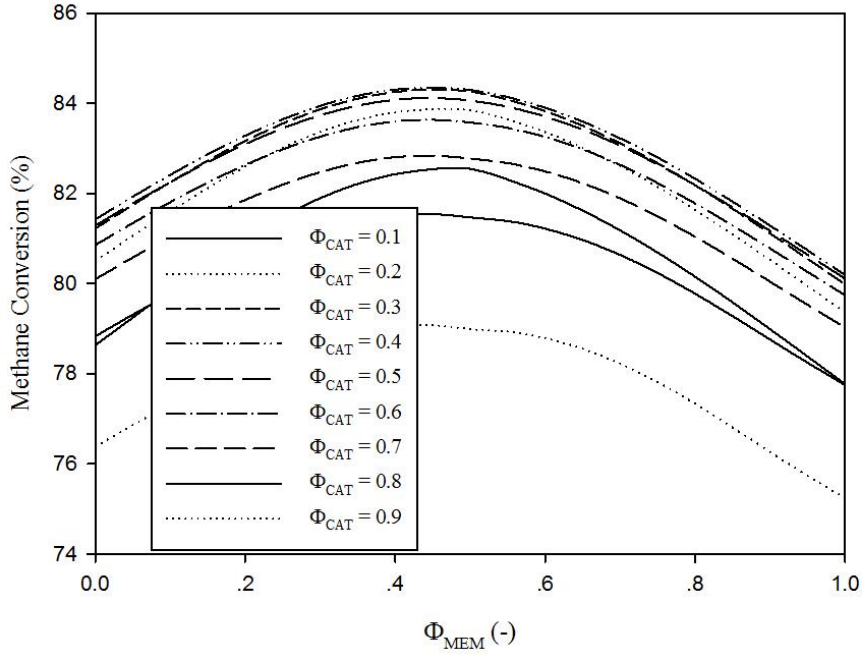

(c) log(*Da*) = 4.489, log(*Pe*) = -3.006

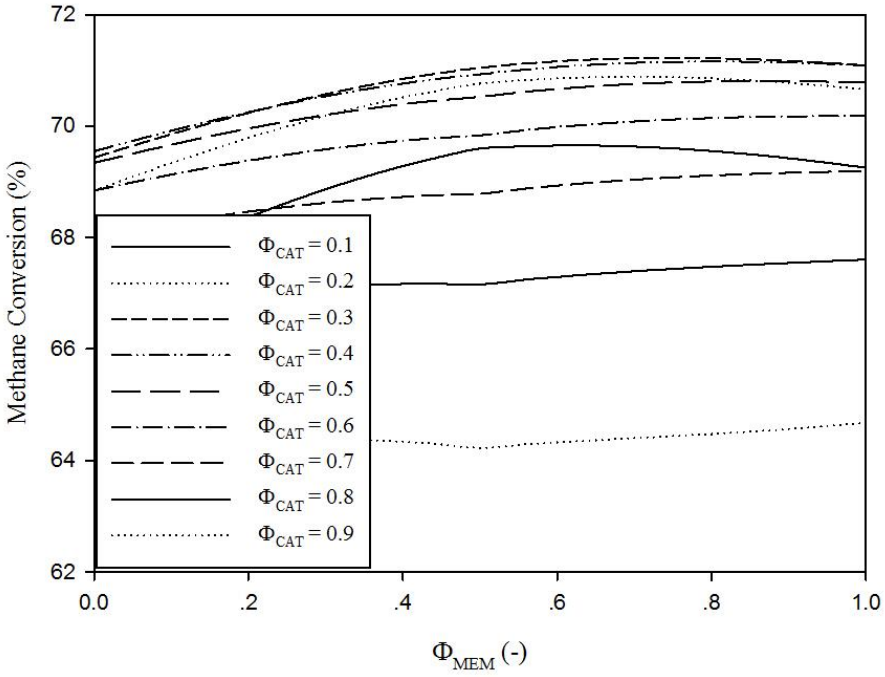

(d) log(*Da*) = 4.489, log(*Pe*) = -2.313

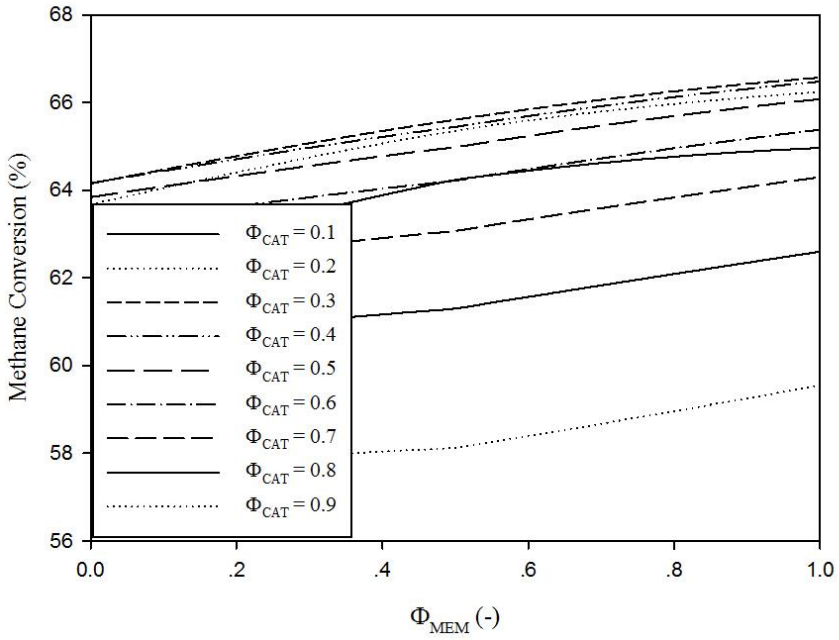

(e) log(*Da*) = 4.489, log(*Pe*) = -1.908

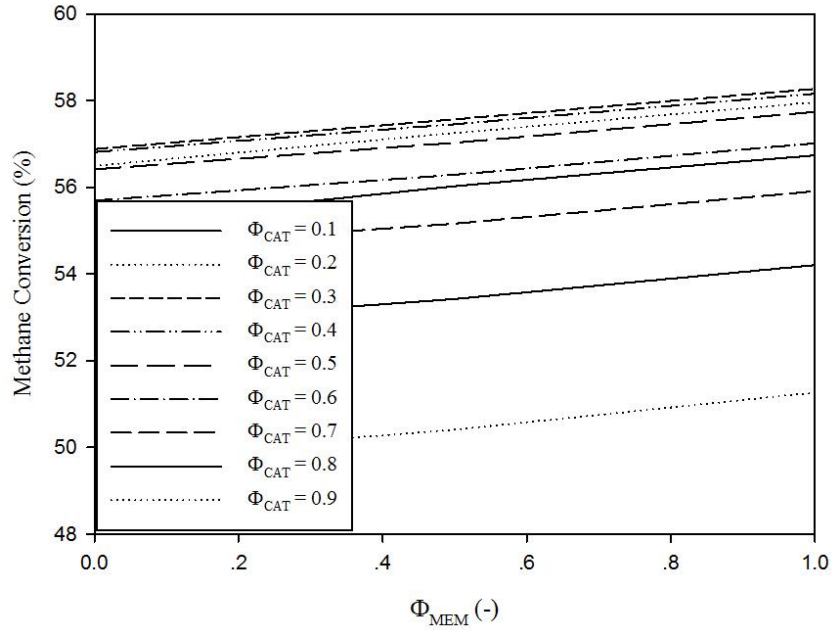

(f) log(*Da*) = 4.489, log(*Pe*) = -0.704

Figure 5.19 Methane conversion at the reactor exit of non-uniform distribution membrane reactor at different *Pe* and constant *Da*

Figure 5.19 showed methane conversion at the exit of non-uniform distribution and uniform distribution membrane reactors with different *Pe* number. For the non-uniform distribution considered in Fig. 5.19, Damkohler number was kept to be constant at 4.489. The results showed that, at high *Pe* number (low H_2 permeation rate), maximum methane conversion was achieved as membrane fraction at the 1st section of membrane reactor was equal to 1. Also, membrane reactor with lower catalyst fraction at the 1st reactor section always offered higher methane conversion compared to the uniform distribution membrane reactor and reactor configuration with higher catalyst fraction at the 1st reactor section because of higher achieved temperature of the former one compared to the two latter ones at the 1st reactor section.

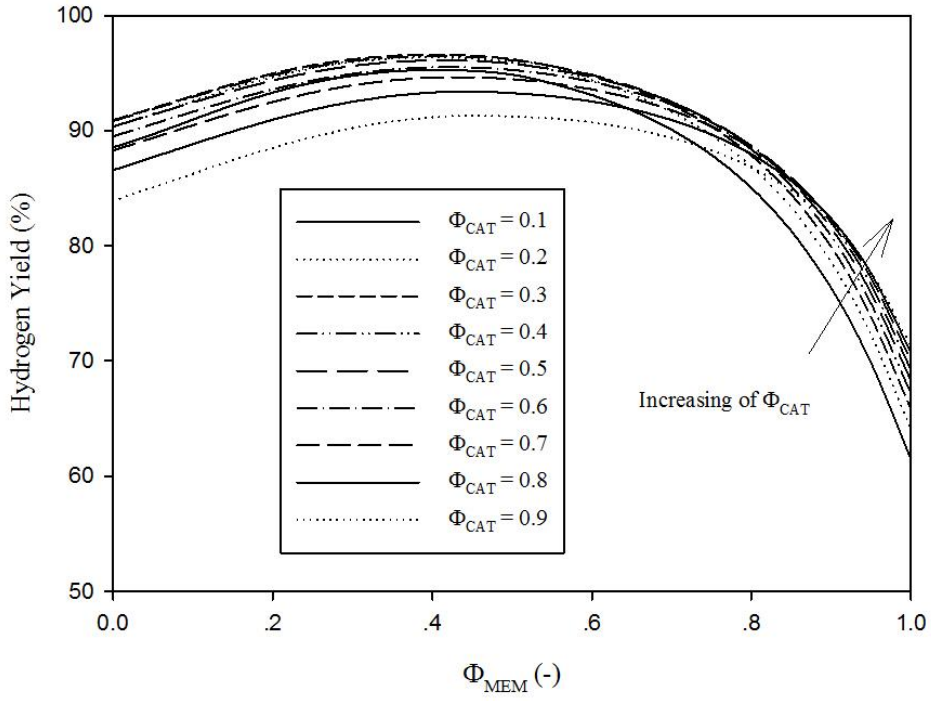

(a) log(*Da*) = 4.489, log(*Pe*) = -3.699

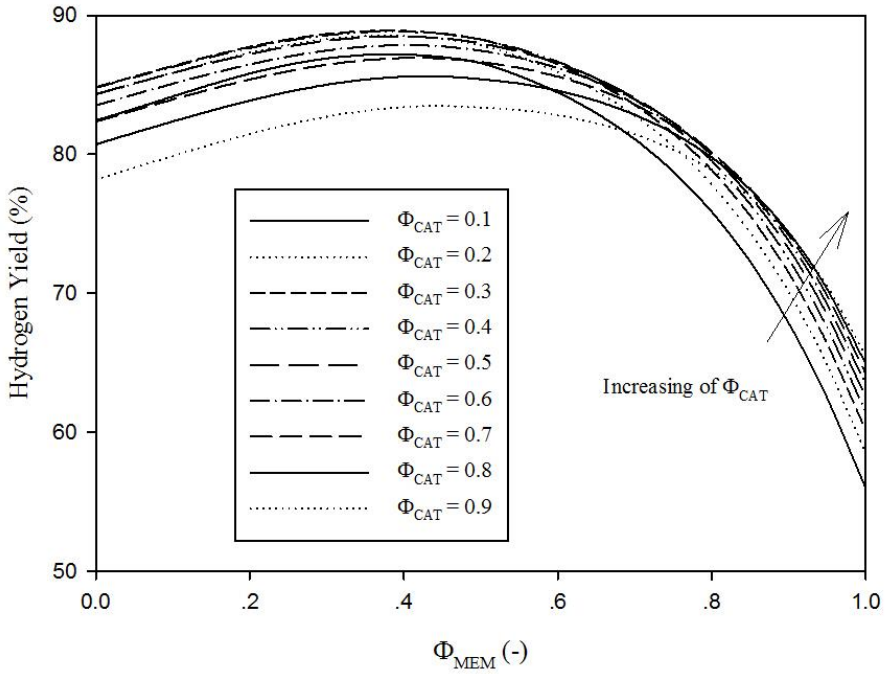

(b) log(*Da*) = 4.489, log(*Pe*) = -3.412

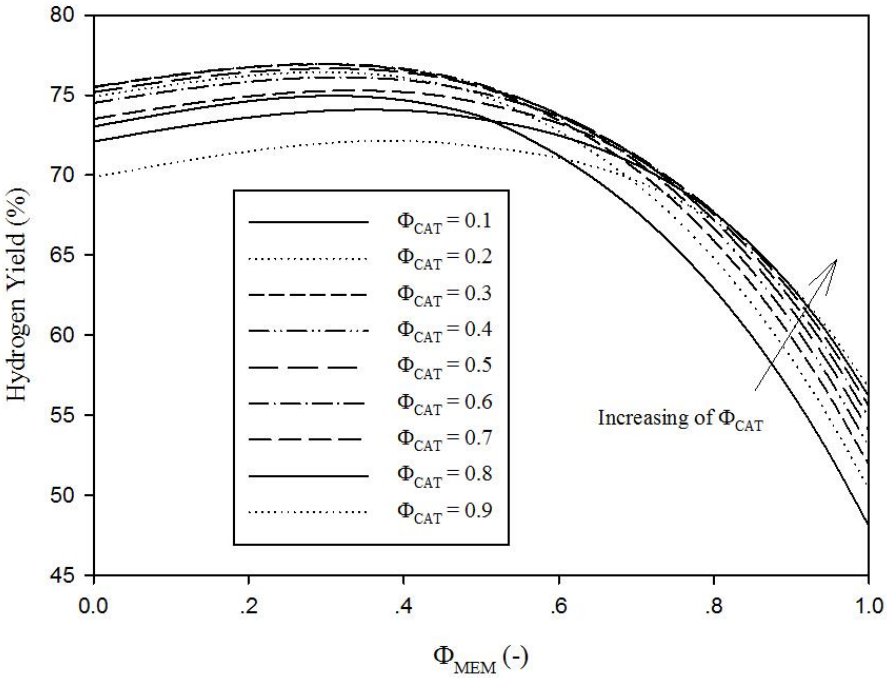

(c) log(*Da*) = 4.489, log(*Pe*) = -3.006

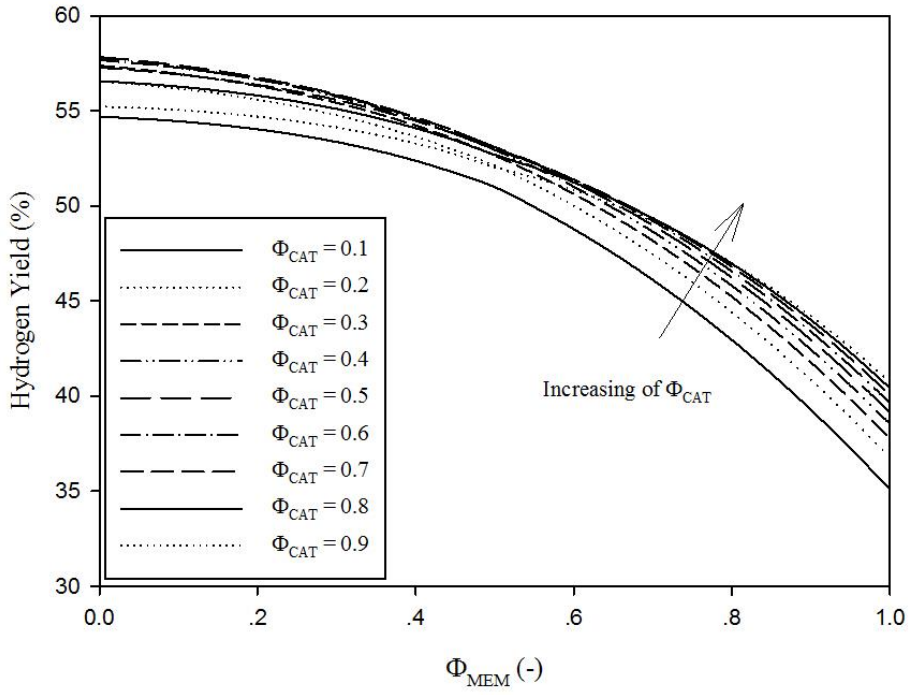

(d) log(*Da*) = 4.489, log(*Pe*) = -2.313

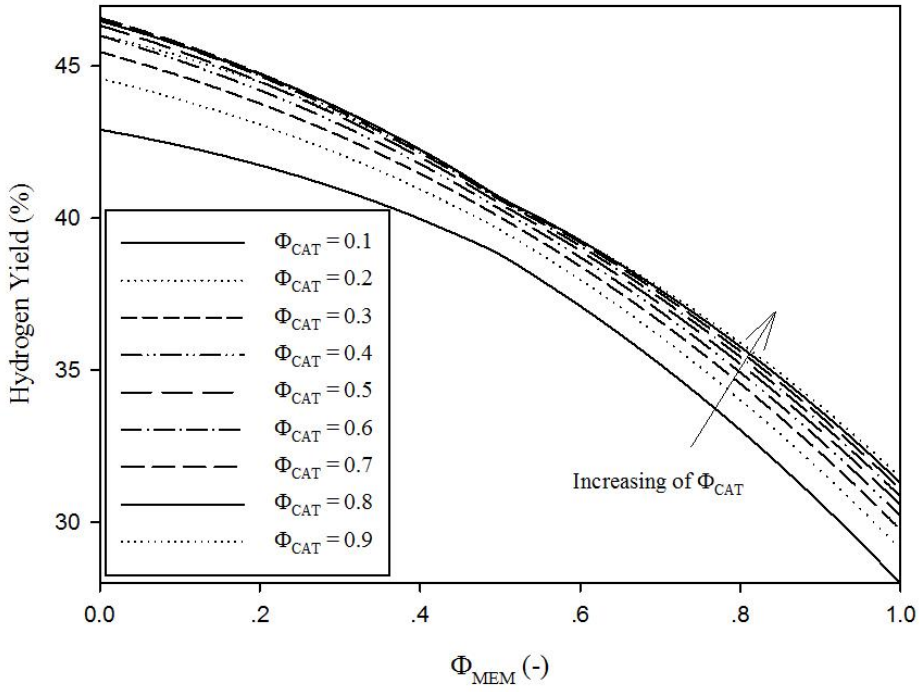

(e) log(*Da*) = 4.489, log(*Pe*) = -1.908

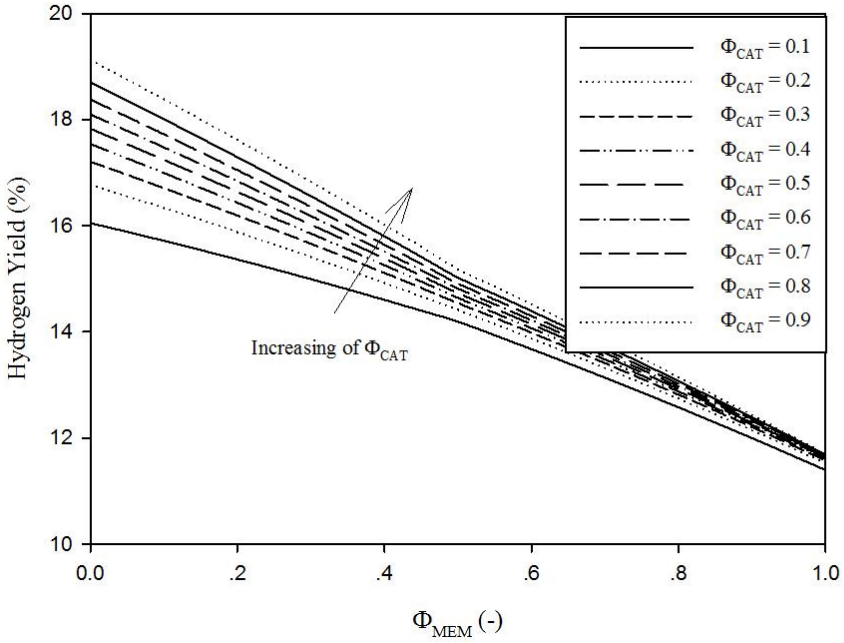

(f) log(*Da*) = 4.489, log(*Pe*) = -0.704

Figure 5.20 H_2 yield at the reactor exit of non-uniform distribution membrane reactor at different *Pe* and constant *Da*

Figure 5.20 showed hydrogen yield at the exit of non-uniform distribution and uniform distribution membrane reactors with different *Pe* number. For the consideration in Fig. 5.20, Damkohler number was kept to be constant at 4.489. The results showed that, for low H_2 permeability (high *Pe* number), the maximum of hydrogen yield would be obtained when the fraction of membrane area at the 1st section approached to 0. For non-uniform distribution membrane reactor with high *Pe* number (low H_2 permeability), higher catalyst fraction at the 1st section could offer maximum hydrogen yield because of higher retention time for generated H_2 to permeate through membrane.

To evaluate and optimize the configuration of non-uniform distribution membrane reactor, the conventional membrane reactor was considered as a base case. In this study, the conventional membrane reactor at different total catalyst density (*Da* number) and H_2 permeation rate (*Pe* number) which offered 97% of methane conversion was considered as a base case for performance benchmarking as shown in Figs. 5.21. The fractions of

catalyst packing and membrane area at the 1st section were varied to investigate the improvement of methane conversion.

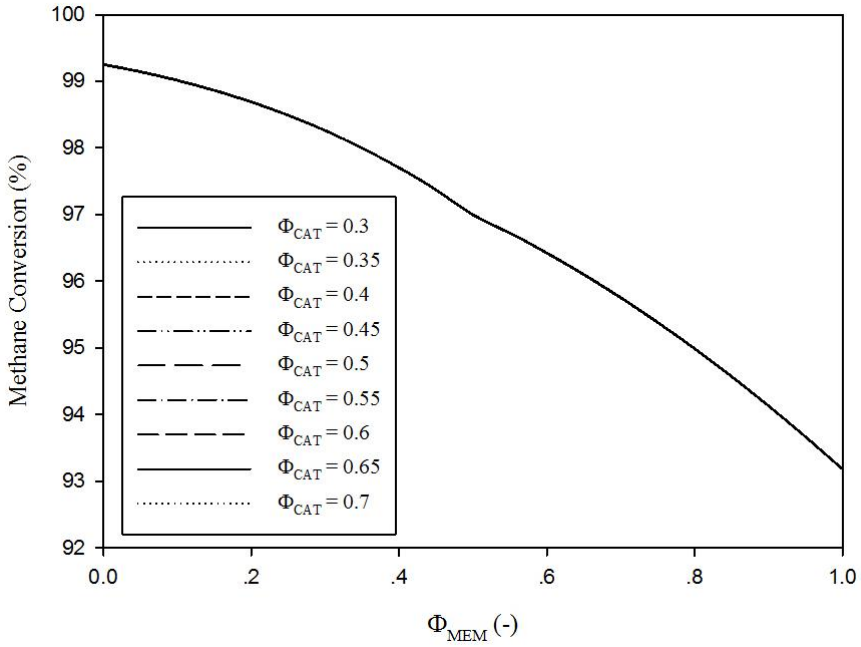

(a) log(*Da*) = 12.090, log(*Pe*) = -2.784

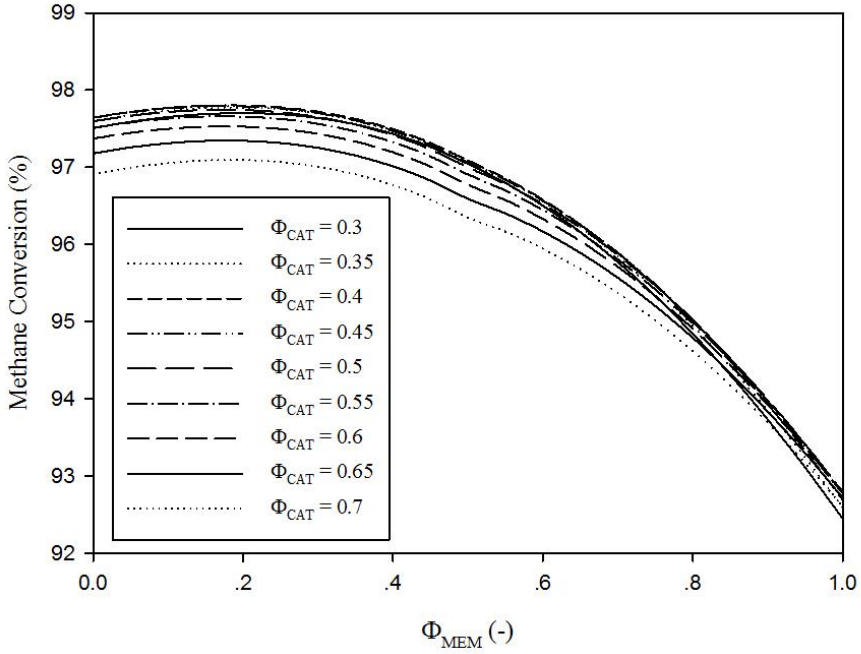

(b) log(*Da*) = 7.485, log(*Pe*) = -2.938

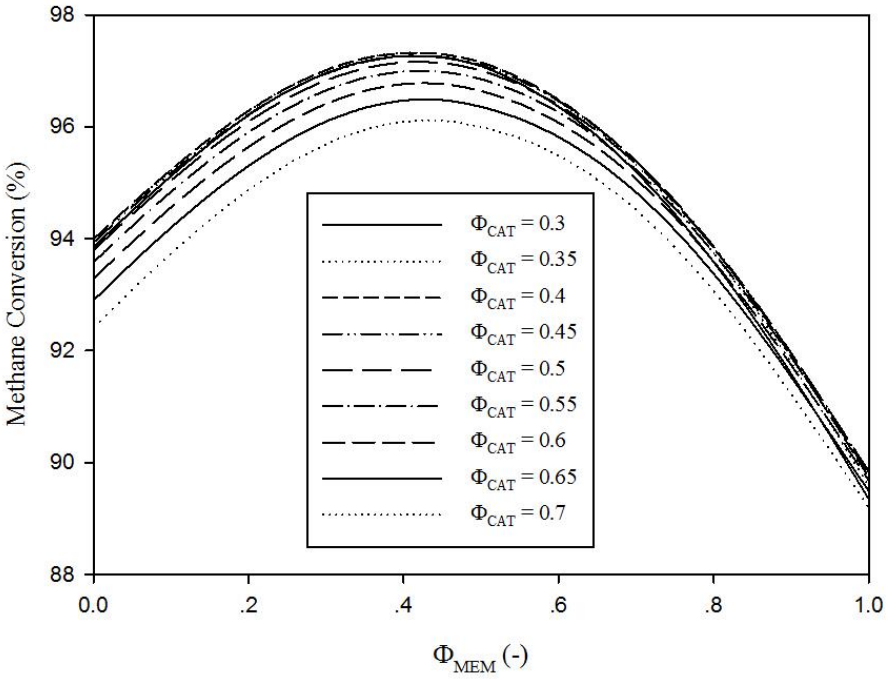

(c) log(*Da*) = 5.182, log(*Pe*) = -3.400

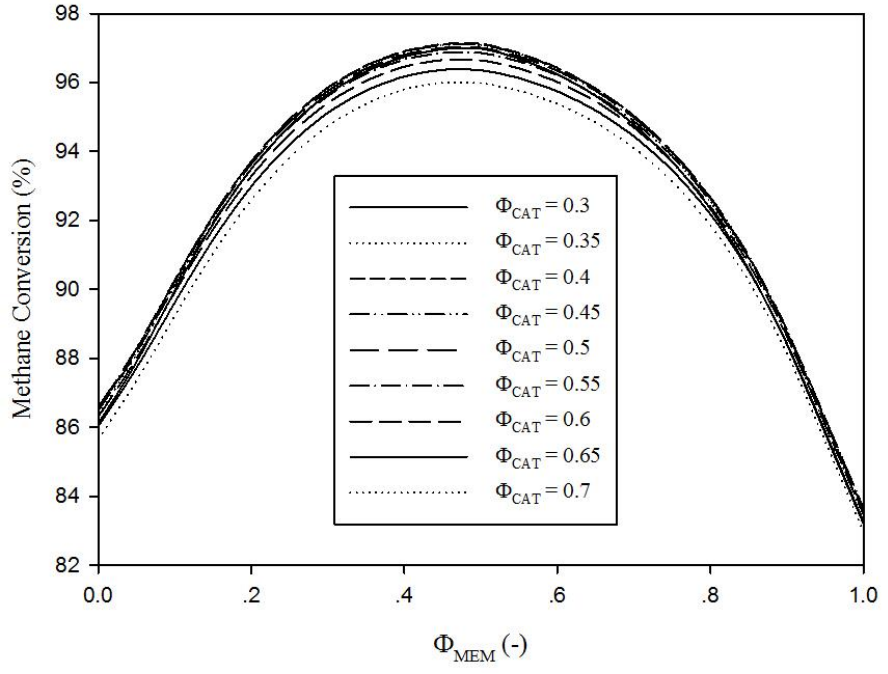

(d) log(*Da*) = 2.880, log(*Pe*) = -4.017

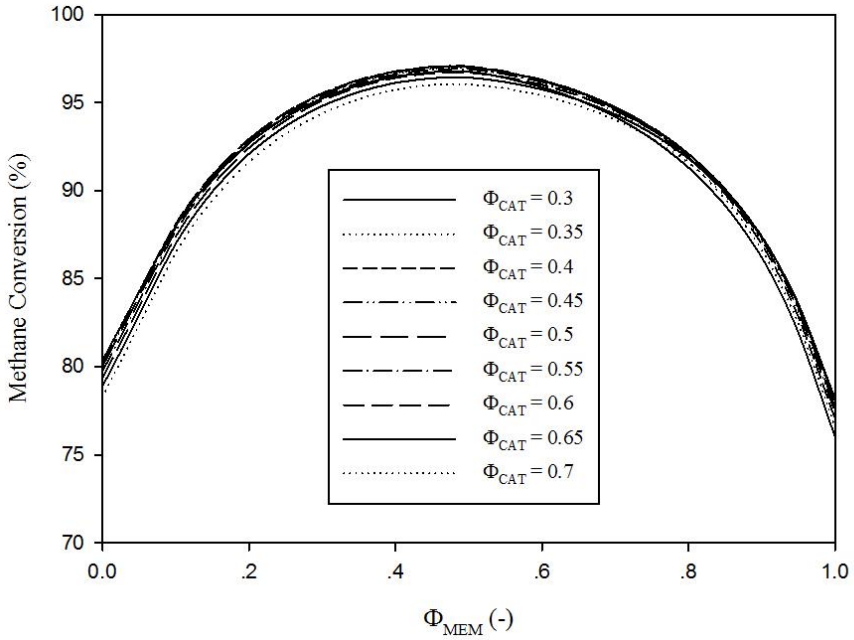

(e) log(*Da*) = 0.577, log(*Pe*) = -4.674

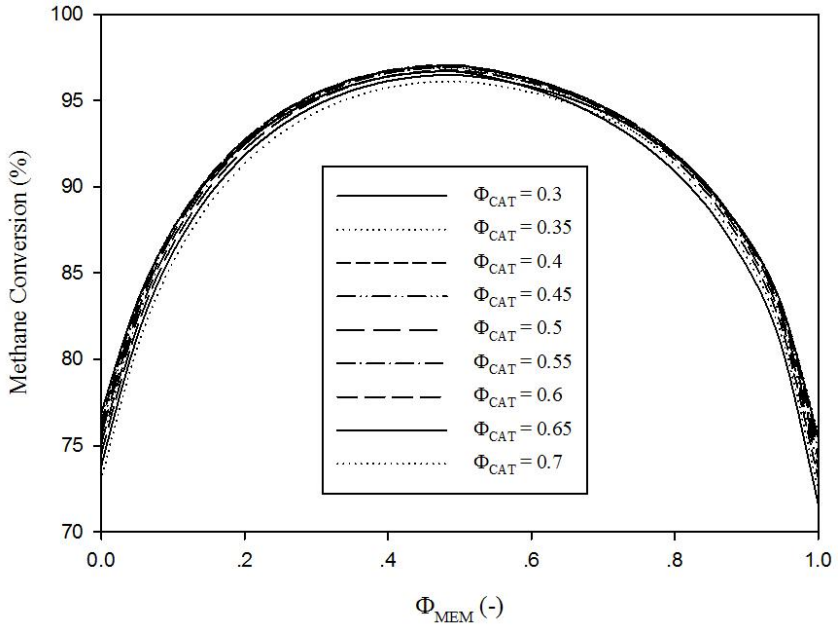

(f) log(*Da*) = -1.726, log(*Pe*) = -5.411

Figure 5.21 Methane conversion at the reactor exit of non-uniform distribution membrane reactor that total catalyst density and membrane area were adjusted until methane conversion of conventional membrane reactor was equal to 97%

As shown in Figs. 5.21, it could be concluded that maximum methane conversion of non-uniform distribution membrane reactor was achieved, when the catalyst density and membrane area at the 1st reactor section were lower than those at the 2nd reactor section. The membrane reactor which log(*Da*) = 12.090, log(*Pe*) = -2.784, offered the largest difference of methane conversion between non-uniform distribution membrane reactor with optimum configuration and uniform distribution membrane reactor. With this *Da* and *Pe* numbers, over 99% methane conversion could be achieved as the catalyst and membrane fraction at the 1st reactor section was equal to 0.5 and 0, respectively. The performance evaluation of non-uniform membrane reactor considering the conventional membrane reactor operating at different *Da* number and *Pe* number which offered H_2 yield of 85% was also performed as shown in Figs. 5.22.

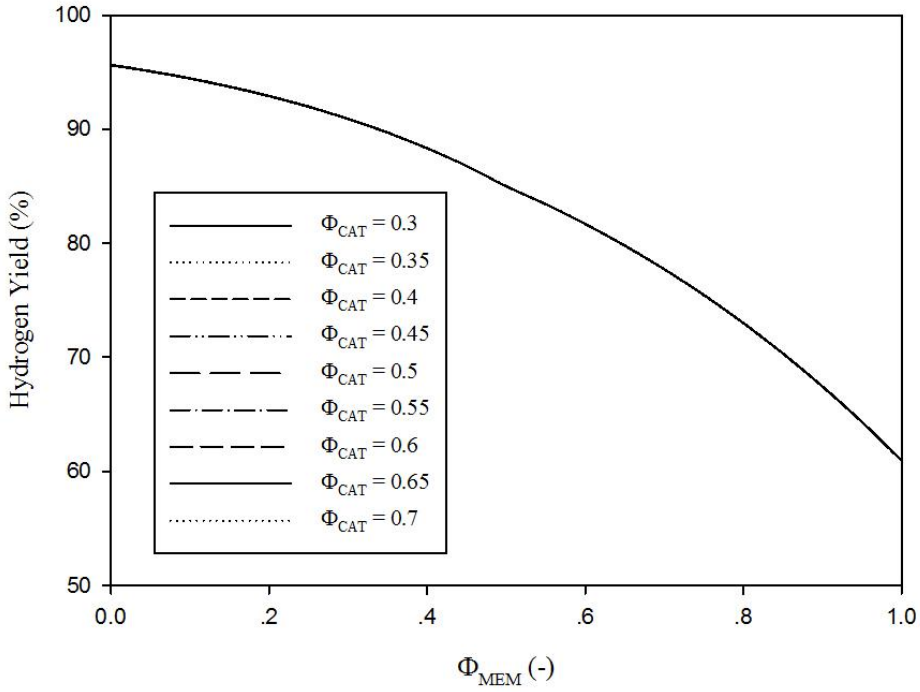

(a) log(*Da*) = 12.090, log(*Pe*) = -2.878

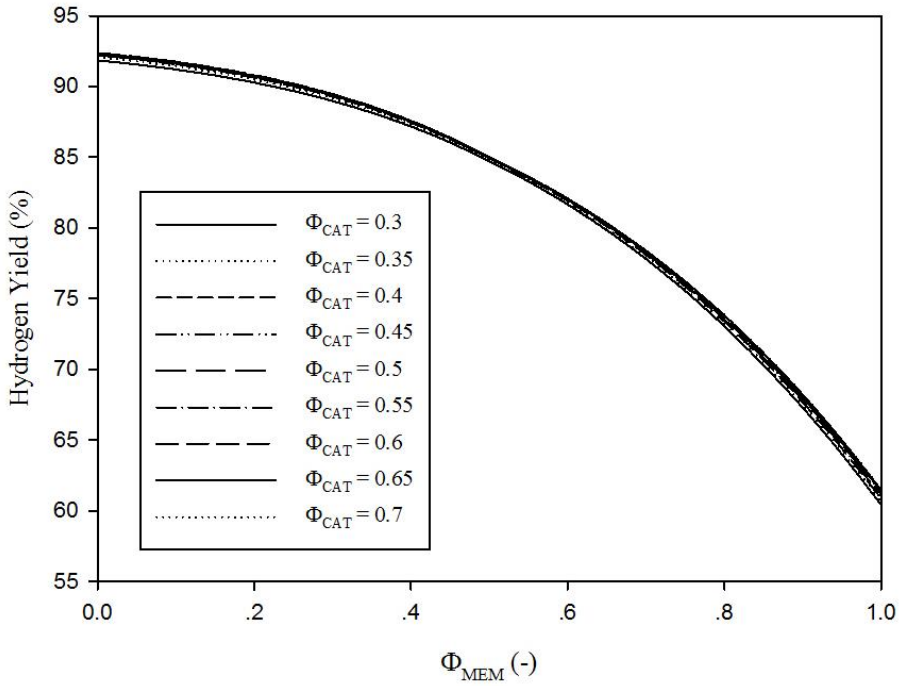

(b) log(*Da*) = 7.485, log(*Pe*) = -2.914

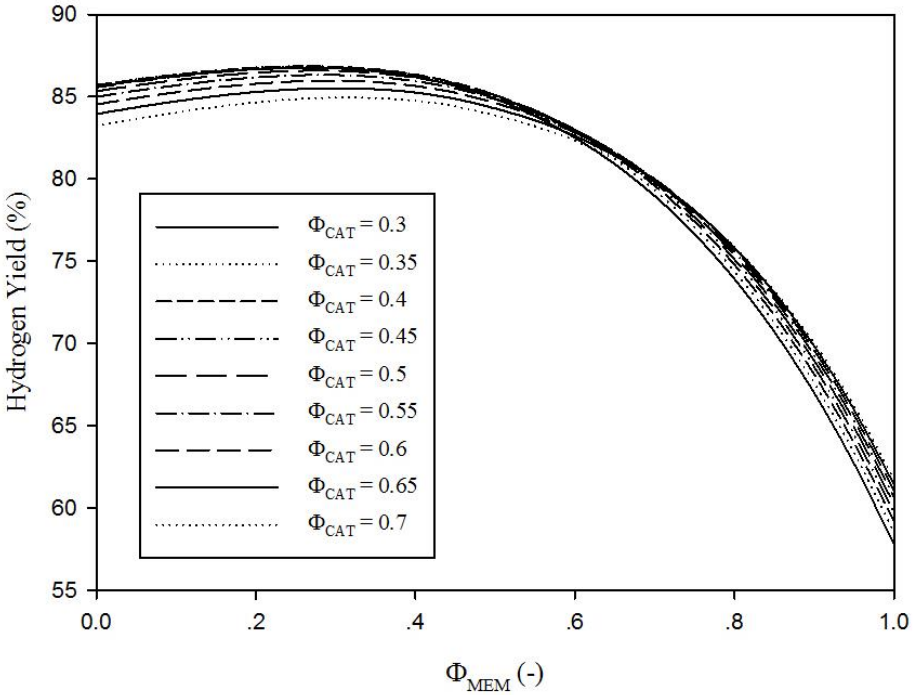

(c) log(*Da*) = 5.182, log(*Pe*) = -3.415

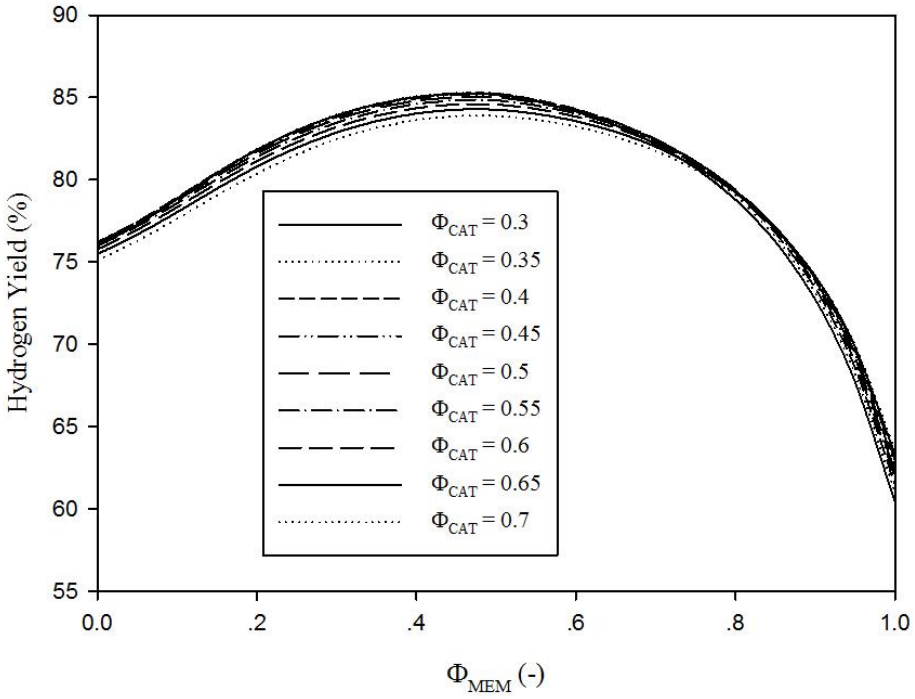

(d) log(*Da*) = 2.880, log(*Pe*) = -3.736

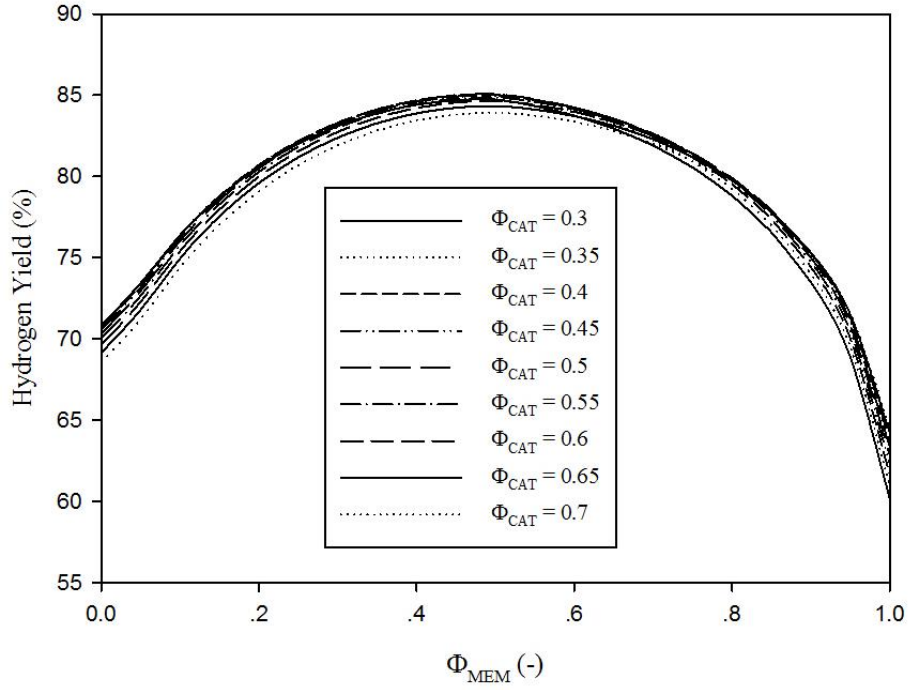

(e) log(*Da*) = 0.577, log(*Pe*) = -4.277

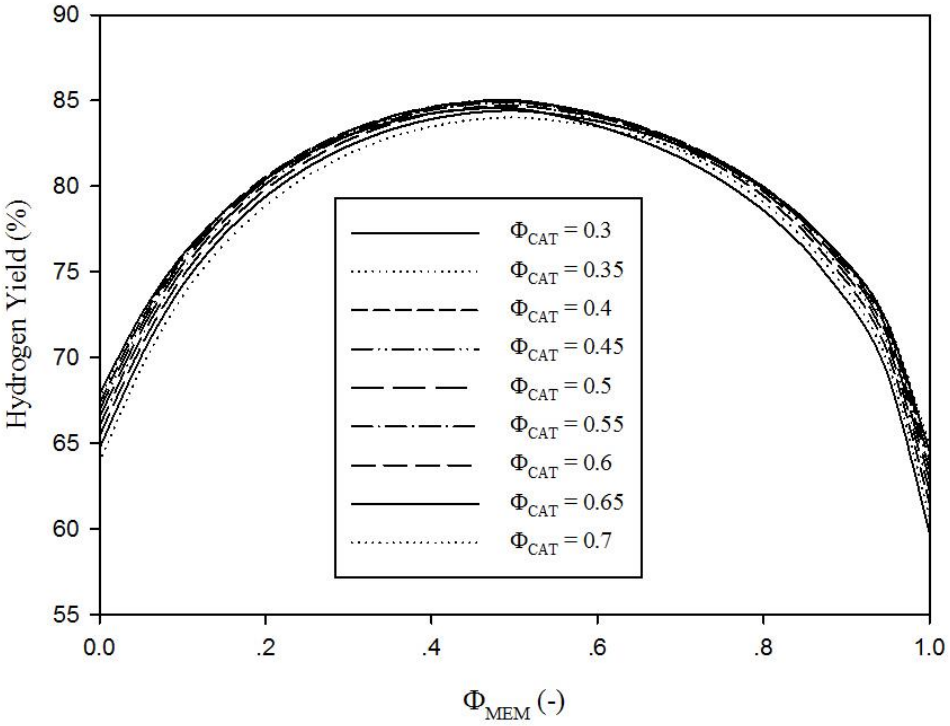

(f) log(*Da*) = -1.726, log(*Pe*) = -4.962

Figure 5.22 H_2 yield at the reactor exit of non-uniform distribution membrane reactor that total catalyst density and membrane area were adjusted until H_2 yield of conventional membrane reactor was equal to 85%

The results from Figs. 5.22 indicated that non-uniform distribution membrane reactor could also offer maximum hydrogen yield when the catalyst density and membrane area at the 1st reactor section were lower than those at the 2nd reactor section. Non-uniform distribution membrane reactor could significantly offer higher H_2 yield compared to uniform distribution membrane reactor at high values of *Da* and *Pe* numbers (log(*Da*) = 12.090, log(*Pe*) = -2.878). More than 95% of H_2 yield could be achieved for the non-uniform distribution membrane reactor as the fractions of catalyst packing and membrane area were in the 1st reactor section was equal to 0.55 and 0, respectively.

According to the simulation results, it could be concluded that to the optimum performance of membrane reactor, with the reactor dimensions considered in this study, was achieved as the catalyst weight was more than 0.9146 kg, and the value of membrane area to membrane thickness ratio was between 7,543 and 9,425 m.

CHAPTER VI

CONCLUSION AND RECOMMENDATION

6.1 Conclusion

The membrane reactor was one of the multifunctional reactors which combined the reaction and separation functions into the same unit. This reactor type could be applied in H_2 generation via steam methane reforming reaction in order to improve higher methane conversion and hydrogen yield. Moreover, high-purity hydrogen could be achieved for steam methane reforming in membrane reactor. Normally, a conventional membrane reactor contained catalyst and membrane which was uniform distributed along the reactor length. The disadvantage of this configuration was useless membrane reactor in the starting path because of low concentration of hydrogen and extreme temperature drop due to the endothermic steam reforming reaction at that reactor position.

In this study, to resolve the issue above, the membrane reactor was divided into two sections with different amount of catalyst packing and membrane area. For every scenario considered in this study, the total catalyst density and membrane area were controlled at the constant values. Hydrogen yield and methane conversion were considered as the performance indicator in this work. The results showed that as the membrane fraction of non-uniform distribution membrane reactor at the 1^{st} reactor section was more than the 2^{nd} reactor section, its temperature and hydrogen partial pressure at the retentate chamber were lower than uniform distribution membrane reactor in the 1^{st} reactor section, but the inverse trend was observed at the 2^{nd} reactor section. If the catalyst fraction in the 1^{st} reactor section was higher than the 2^{nd} section, temperature of non-uniform distribution membrane reactor was lower than uniform distribution membrane reactor at the 1^{st} reactor section; however, hydrogen partial pressure of the former became higher than the latter in the 1^{st} reactor section. Also, these behaviors were in the opposite direction at the 2^{nd} reactor section.

In order to evaluate the performance of non-uniform distribution membrane reactor and also optimize the its configuration, the effect of Damkohler (*Da*) number, Peclet (*Pe*) number, fraction of catalyst packing and membrane area at the 1^{st} reactor

section on the reactor performance were studied. *Da* number represented the extent of reaction rate, as *Da* number increases, the contribution of reaction increase. *Pe* number represented the extent of H_2 permeation rate. H_2 permeation is enhanced as *Pe* number decreased. For conventional membrane reactor, at high *Pe* number (low H_2 permeation rate), the behavior of membrane reactor was almost similar to conventional reactor. Inversely, if *Da* number was high, the membrane reactor will be controlled by H_2 permeation rate since the reaction rate became relatively high. This phenomenon was called "Permeation limitation".

For the evaluation of non-uniform distribution membrane reactor, methane conversion and hydrogen yield at the reactor exit were considered as the performance indicators to determine the best configuration of membrane reactor. The results from this study indicated that, the operation near the permeation limitation, non-uniform distribution membrane reactor could offer significantly higher performance compared to uniform distribution membrane reactor. In cases that *Pe* number (H_2 permeability) was controlled to be constant, as the total amount of catalyst used in the reactor increased, the fraction of membrane area at the 1^{st} reactor section should be decreased in order to maximize the reactor performance. In cases that *Da* number (total amount of catalyst) was kept constant, as *Pe* number increased (H_2 permeability decreased), the value of fraction of membrane area should be low to achieve high reactor performance. For the operation near the permeation limitation zone, the change in catalyst packing distribution did not significantly affect the reactor performance.

In summary, the membrane reactor could effectively perform as it was operated at the permeation limitation zone. At this operation zone, the membrane area to membrane thickness should be determined between 7,543 and 9,425 m, while the catalyst weight should be more than 0.9146 kg.

6.2 Recommendations

Because this work is the conceptual study, it is difficult to apply in the industry scale. Therefore, more complicated simulation should be performed to evaluate the actual performance of non-uniform distribution membrane reactor prior to be used in the industry scale. Two-dimensional or three-dimensional simulations were also high

performance tools used to envision all phenomena inside the membrane reactor, for example the generation of hot spot or cold spot, the hydrodynamics, etc. Moreover, the study of the distribution of catalyst packing might be not required since it did not significantly affect the reactor performance. Also, since the number of section of non-uniform distribution membrane reactor considered in this study is two, the optimum section number of non-uniform distribution membrane reactor should be further studied.

REFERENCES

[1] Chiappetta, G., Clarizia, G. ,and Drioli, E. Theoretical analysis of the effect of catalyst mass distribution and operation parameters on the performance of a Pd-based membrane reactor for water–gas shift reaction. Chemical Engineering Journal 136 (2008): 373-382.

[2] Basile, A. Hydrogen Production Using Pd-based Membrane Reactors for Fuel Cells. Topics in Catalysis 51 (2008): 107-122.

[3] Bayat, M. ,and Rahimpour, M. R. Production of hydrogen and methanol enhancement via a novel optimized thermally coupled two-membrane reactor. International Journal of Energy Research 37 (2013): 105-120.

[4] Kothari, R., Buddhi, D. ,and Sawhney, R. L. Comparison of environmental and economic aspects of various hydrogen production methods. Renewable and Sustainable Energy Reviews 12 (2008): 553-563.

[5] Barbieri, G., Brunetti, A., Caravella, A. ,and Drioli, E. Pd-based membrane reactors for one-stage process of water gas shift. RSC Advances 1 (2011): 651.

[6] Caravella, A., Di Maio, F. P. ,and Di Renzo, A. Optimization of membrane area and catalyst distribution in a permeative-stage membrane reactor for methane steam reforming. Journal of Membrane Science 321 (2008): 209-221.

[7] Piemonte, V., De Falco, M., Favetta, B. ,and Basile, A. Counter-current membrane reactor for WGS process: Membrane design. International Journal of Hydrogen Energy 35 (2010): 12609-12617.

[8] Hohn, K. L. ,and Schmidt, L. D. Partial oxidation of methane to syngas at high space velocities over Rh-coated spheres. Applied Catalysis A: General 211 (2001): 53-68.

[9] Holladay, J. D., Hu, J., King, D. L. ,and Wang, Y. An overview of hydrogen production technologies. Catalysis Today 139 (2009): 244-260.

[10] Song, C. Fuel processing for low-temperature and high-temperature fuel cells: Challenges, and opportunities for sustainable development in the 21st century. Catalysis Today 77 (2002): 17-49.

[11] Krummenacher, J. Catalytic partial oxidation of higher hydrocarbons at millisecond contact times: decane, hexadecane, and diesel fuel. Journal of Catalysis 215 (2003): 332-343.

[12] Carmo, M., Fritz, D. L., Mergel, J. ,and Stolten, D. A comprehensive review on PEM water electrolysis. International Journal of Hydrogen Energy 38 (2013): 4901-4934.

[13] Takata, H., Mizuno, N., Nishikawa, M., Fukada, S. ,and Yoshitake, M. Adsorption properties of water vapor on sulfonated perfluoropolymer membranes. International Journal of Hydrogen Energy 32 (2007): 371-379.

[14] Marigliano, G., Barbieri, G. ,and Drioli, E. Effect of energy transport on a palladium-based membrane reactor for methane steam reforming process. Catalysis Today 67 (2001): 85-99.

[15] Cser, L., Torok, G., Krexner, G., Prem, M. ,and Sharkov, I. Neutron holographic study of palladium hydride. Applied Physics Letters 85 (2004): 1149-1151.

[16] Narehood, D., et al. X-ray diffraction and H-storage in ultra-small palladium particles. International Journal of Hydrogen Energy 34 (2009): 952-960.

[17] Ayturk, M. E. ,and Ma, Y. H. Electroless Pd and Ag deposition kinetics of the composite Pd and Pd/Ag membranes synthesized from agitated plating baths. Journal of Membrane Science 330 (2009): 233-245.

[18] Brodowsky, H. The Palladium Hydrogen System. Von F. A. Lewis, Academic Press, London-New York 1967. 1. Aufl., XII, 178 S., zahlr. Abb., geb. 45 s. Angewandte Chemie 80 (1968): 498-498.

[19] Ohira, K., Sakamoto, Y. ,and Flanagan, T. B. Thermodynamic properties for solution of hydrogen in Pd-Ag-Ni ternary alloys. Journal of Alloys and Compounds 236 (1996): 42-49.

[20] Rogers, H. C. Hydrogen Embrittlement of Metals: Atomic hydrogen from a variety of sources reduces the ductility of many metals. Science 159 (1968): 1057-1064.

[21] Collins, J. P., et al. Catalytic Dehydrogenation of Propane in Hydrogen Permselective Membrane Reactors. Industrial & Engineering Chemistry Research 35 (1996): 4398-4405.

[22] Gallucci, F., Defalco, M., Tosti, S., Marrelli, L. ,and Basile, A. The effect of the hydrogen flux pressure and temperature dependence factors on the membrane reactor performances. International Journal of Hydrogen Energy 32 (2007): 4052-4058.

[23] Yun, S. ,and Ted Oyama, S. Correlations in palladium membranes for hydrogen separation: A review. Journal of Membrane Science 375 (2011): 28-45.

[24] Tosti, S. Overview of Pd-based membranes for producing pure hydrogen and state of art at ENEA laboratories. International Journal of Hydrogen Energy 35 (2010): 12650-12659.

[25] Xu, J. ,and Froment, G. F. Methane steam reforming, methanation and water-gas shift: I. Intrinsic kinetics. AIChE Journal 35 (1989): 88-96.

[26] Yu, W. A comparative simulation study of methane steam reforming in a porous ceramic membrane reactor using nitrogen and steam as sweep gases. International Journal of Hydrogen Energy 33 (2008): 685-692.

[27] Moon, W. S. ,and Park, S. B. Design guide of a membrane for a membrane reactor in terms of permeability and selectivity. Journal of Membrane Science 170 (2000): 43-51.

[28] Boutikos, P. ,and Nikolakis, V. A simulation study of the effect of operating and design parameters on the performance of a water gas shift membrane reactor. Journal of Membrane Science 350 (2010): 378-386.

[29] Gómez-García, M. Á., Dobrosz-Gómez, I., Fontalvo, J. ,and Rynkowski, J. M. Membrane reactor design guidelines for ammonia decomposition. Catalysis Today 191 (2012): 165-168.

[30] Chiappetta, G., Barbieri, G. ,and Drioli, E. Pd/Ag-based membrane reactors on small scale: Assessment of the feed pressure and design parameters effect on the performance. Chemical Engineering and Processing: Process Intensification 49 (2010): 722-731.

[31] Lin, Y.-M., Liu, S.-L., Chuang, C.-H. ,and Chu, Y.-T. Effect of incipient removal of hydrogen through palladium membrane on the conversion of methane steam reforming. Catalysis Today 82 (2003): 127-139.

[32] Mendes, D., et al. Experimental and modeling studies on the low-temperature water-gas shift reaction in a dense Pd–Ag packed-bed membrane reactor. Chemical Engineering Science 66 (2011): 2356-2367.

[33] Lima, F. V., Daoutidis, P., Tsapatsis, M. ,and Marano, J. J. Modeling and Optimization of Membrane Reactors for Carbon Capture in Integrated Gasification Combined Cycle Units. Industrial & Engineering Chemistry Research 51 (2012): 5480-5489.

[34] Barbieri, G., Brunetti, A., Tricoli, G. ,and Drioli, E. An innovative configuration of a Pd-based membrane reactor for the production of pure hydrogen. Journal of Power Sources 182 (2008): 160-167.

[35] Li, A., Lim, C. J. ,and Grace, J. R. Staged-separation membrane reactor for steam methane reforming. Chemical Engineering Journal 138 (2008): 452-459.

[36] Li, A., Lim, C. J., Boyd, T. ,and Grace, J. R. Simulation of autothermal reforming in a staged-separation membrane reactor for pure hydrogen production. The Canadian Journal of Chemical Engineering 86 (2008): 387-394.

[37] Hwang, S. ,and Smith, R. Heterogeneous catalytic reactor design with optimum temperature profile I: application of catalyst dilution and side-stream distribution. Chemical Engineering Science 59 (2004): 4229-4243.

[38] Caravella, A., Di Maio, F. P. ,and Di Renzo, A. Computational study of staged membrane reactor configurations for methane steam reforming. I. Optimization of stage lengths. AIChE Journal 56 (2010): 248-258.

[39] Caravella, A., Di Maio, F. P. ,and Di Renzo, A. Computational study of staged membrane reactor configurations for methane steam reforming. II. Effect of number of stages and catalyst amount. AIChE Journal 56 (2010): 259-267.

[40] Gallucci, F., Paturzo, L., Famà, A. ,and Basile, A. Experimental Study of the Methane Steam Reforming Reaction in a Dense Pd/Ag Membrane Reactor. Industrial & Engineering Chemistry Research 43 (2004): 928-933.

[41] Kikuchi, E. Membrane reactor application to hydrogen production. Catalysis Today 56 (2000): 97-101.

[42] Oyama, S. T. ,and Lim, H. An operability level coefficient (OLC) as a useful tool for correlating the performance of membrane reactors. Chemical Engineering Journal 151 (2009): 351-358.

APPENDIX

APPENDIX A

- Specific heat capacity: the dependence of specific heat of a single component on temperature was;

$Cp_{CH_4} = 4.18(5.34 + 0.0115 \cdot T)$ kJ/kmol K

$Cp_{H_2O} = 4.18(8.22 + 0.000115 \cdot T + 1.34 \times 10^{-6} \cdot T^2)$ kJ/kmol K

$Cp_{CO} = 4.18(6.6 + 0.0012 \cdot T)$ kJ/kmol K

$Cp_{CO_2} = 4.18(10.34 + 0.00274 \cdot T - 195500 \cdot T^{-2})$ kJ/kmol K

$Cp_{H_2} = 4.18(6.62 + 0.00081 \cdot T)$ KJ/kmol K

- Heat of reaction

$\Delta H_I = 206310 + \int_{298}^{T} (3Cp_{H_2} + Cp_{CO} - Cp_{CH_4} - Cp_{H_2O}) dT$ kJ/kmol

$\Delta H_{III} = 1651100 + \int_{298}^{T} (4Cp_{H_2} + Cp_{CO_2} - Cp_{CH_4} - 2Cp_{H_2O}) dT$ KJ/kmol

$\Delta H_{II} = \Delta H_{III} - \Delta H_I$ kJ/kmol

VITA

Mr. Akkarapon Cheevataranakorn was born in Phuket province, Thailand, on December 29, 1988. He finished high school from Phuketwittayalai School, Phuket, Thailand, 2007. He received his Bachelor Degree in Chemical Engineering from King Mongkut's University of Technology Thonburi in Year 2011. He was now studying Master Degree at Department of Chemical Engineering, Faculty of Engineering, Chulalongkorn University, Thailand.